UNCLASSIFIED

AD NUMBER

AD 152 952

CLASSIFICATION CHANGES

TO **UNCLASSIFIED**

FROM **CONFIDENTIAL**

AUTHORITY

USABRL; Apr 22, 1981.

19990303117

THIS PAGE IS UNCLASSIFIED

UNCLASSIFIED

AD NUMBER

AD-152 952

NEW LIMITATION CHANGE

TO

DISTRIBUTION STATEMENT - A

Approved for public release;
distribution is unlimited.

LIMITATION CODE: 1

FROM

No Predecessor DoD Distr Scty Cntrl St'mt Assigned

AUTHORITY

USABRL, Apr 22, 1981

THIS PAGE IS UNCLASSIFIED

[redacted]

BRL

FC

MEMORANDUM REPORT No. 1098

AUGUST 1957

Aerodynamic Characteristics Of 30-mm HEI Shell, T306 E10 (U)

EUGENE T. ROECKER

EUGENE D. BOYER

DEPARTMENT OF THE ARMY PROJECT No. 5B03-03-001
ORDNANCE RESEARCH AND DEVELOPMENT PROJECT No. TB3-0108

BALLISTIC RESEARCH LABORATORIES

ABERDEEN PROVING GROUND, MARYLAND

[redacted]

[redacted]L

BALLISTIC RESEARCH LABORATORIES

MEMORANDUM REPORT NO. 1096

AUGUST 1957

THIS REPORT SUPERSEDES BRL TECHNICAL NOTE NO. 896

AERODYNAMIC CHARACTERISTICS OF 30-MM HEI SHELL, T306 E10 (U)

Eugene T. Roecker

Eugene D. Boyer

Department of the Army Project No. 5B03-03-001,
Ordnance Research and Development Project No. TB3-0108

[illegible] 943

ABERDEEN PROVING GROUND, MARYLAND

[redacted]

[redacted]

TABLE OF CONTENTS

[redacted]

[redacted]

B A L L I S T I C   R E S E A R C H   L A B O R A T O R I E S

MEMORANDUM REPORT NO. 1098

ETRoecker/EDBoyer/eeb
Aberdeen Proving Ground, Md.
August 1957

AERODYNAMIC CHARACTERISTICS OF 30-MM HEI SHELL, T306 E10 (U)

ABSTRACT

The aerodynamic properties at small yaws for Mach numbers between 0.5 and 3.0 of the 30-mm HEI, T306 E10 shell as determined by spark range firings are presented and discussed. Particular attention is given to the markedly nonlinear behavior of the Magnus moment for very small yaws and to the reduction in size of the nutational yaw damping rate due to the presence of the arming ball rotor in the fuze. This report supersedes BRL TN 896.

[redacted]

TABLE OF SYMBOLS AND COEFFICIENTS

A	= Axial moment of inertia
B	= Transverse moment of inertia
a	= Intercept of Q function $(Q = a + bM)$
b	= Slope of Q function $(Q = a + bM)$
cm	= Center of Mass
CP_N	= Center of pressure of normal force
d	= Diameter
k_1	= Axial radius of gyration
k_2	= Transverse radius of gyration
K_{10}	= Size of nutational yaw arm at mid-range
K_{20}	= Size of precessional yaw arm at mid-range
K_D	$= (\text{Drag force})/\rho\, u^2 d^2 = K_{D_0} + K_{D_{\delta^2}}\, \delta^2$
k_L	$= (\text{Lift force})/\rho\, u^2 d^2 = (K_{L_0} + K_{L_{\delta^2}}\, \delta^2)\, \delta = K_L \delta$
k_M	$= (\text{Overturning moment}) \,/\, \rho\, u^2 d^3 = (K_{M_0} + K_{M_{\delta^2}}\, \delta^2)\, \delta = K_M \delta$
k_T	$= (\text{Magnus moment}) \,/\, \rho\, u^2 d^3 \nu = (K_{T_0} + K_{T_{\delta^2}}\, \delta^2)\, \delta = K_T \delta$
k_H	$= (\text{Damping moment due to cross angular velocity}) \,/\, \rho\, u^2 d^3 =$
	$(K_{H_0} + K_{H_{\delta^2}}\, \delta^2) \dfrac{d\sqrt{\omega_2^2 + \omega_3^2}}{u} = \dfrac{K_H d\sqrt{\omega_2^2 + \omega_3^2}}{u}$
k_{MA}	$= (\text{Damping moment due to cross acceleration})/\rho\, u^2 d^3 =$
	$(K_{MA_0} + K_{MA_{\delta^2}}\, \delta^2) \dfrac{d\sqrt{\dot{u}_2^2 + \dot{u}_3^2}}{u^2} = \dfrac{K_{MA}\, d\sqrt{\dot{u}_2^2 + \dot{u}_3^2}}{u^2}$

$K_{H_\delta 2}^{*}$ $= K_{H_\delta 2} - K_{MA_\delta 2} + \frac{1}{2} K_{MA_0}$

$K_{T_\delta 2}^{*}$ $= K_{T_\delta 2} - \frac{1}{2} K_{T_0}$

M = Mach number

w = Weight

N = Number of yaw stations

N_T = Number of timing stations

Q $= \sqrt{1 + M^2 K_{D_0}} = a + bM$

s = Gyroscopic stability factor

$\bar{s}$ = Dynamic stability factor

S_L = Radius of swerve at mid-range

$\vec{u}$ $= (u_1 u_2 u_3)$ (total velocity vector)*

u $= \left| \vec{u} \right|$

α = Angle of yaw

δ $= \left| \sin \alpha \right| = \sqrt{\dfrac{u_2^2 + u_3^2}{u^2}}$

$\overline{\delta^2}$ = Mean squared yaw

$$\left.\begin{array}{ll} \delta_e^2 & = K_{10}^2 + K_{20}^2 + \dfrac{\phi_1' K_{10}^2 - \phi_2' K_{20}^2}{\phi_1' - \phi_2'} \\ \delta_{e1}^2 & = K_{10}^2 + 2K_{20}^2 \\ \delta_{e2}^2 & = 2K_{10}^2 + K_{20}^2 \end{array}\right\} \text{Effective Squared Yaws}$$

ϵ_S = Error in swerve fit

ϵ_Y = Error in yaw fit

---

*The "one" axis is along the missile's axis of symmetry.

λ_1	=	Damping rate of nutational yaw
λ_2	=	Damping rate of precessional yaw
ν	=	$\frac{\omega_1 d}{u}$
ϕ_1'	=	Turning rate of nutational arm
ϕ_2'	=	Turning rate of precessional arm
ρ	=	Density of air
σ	=	$\sqrt{1 - 1/s}$
ω	=	$(\omega_1 \omega_2 \omega_3)$ total angular velocity
$(\,')$	=	Prime refers to differentiation with respect to distance.
$(\dot{\ })$	=	Dot refers to differentiation with respect to time

RESULTS OF REF. 5

Subscript "range" refers to coefficients computed according to Ref. (b).

$$K_{D_{range}} = K_{D_0} + K_{D_{\delta^2}} \overline{\delta^2}$$

$$K_{L_{range}} = K_{L_0} + K_{L_{\delta^2}} \delta_{e2}^{\ 2}$$

$$K_{M_{range}} = K_{M_0} + K_{M_{\delta^2}} \delta_e^{\ 2}$$

$$(K_H - K_{MA})_{range} = K_{H_0} - K_{MA_0} + K_{H_{\delta^2}}^{*} \left[\frac{\phi_1' K_{20}^{\ 2} - \phi_2' K_{10}^{\ 2}}{\phi_1' - \phi_2'} \right]$$

$$- \frac{B}{A} \left[\frac{\phi_1' + \phi_2'}{\phi_1' - \phi_2'} \right] \left[K_{10}^{\ 2} - K_{20}^{\ 2} \right] K_{T_{\delta^2}}^{*}$$

$$K_{T_{range}} = K_{T_0} + K_{T_{\delta^2}}^{*} \delta_e^{\ 2} + \frac{A}{B} \left[\frac{\phi_1'^2 K_{10}^{\ 2} - \phi_2'^2 K_{20}^{\ 2}}{\phi_1'^2 - \phi_2'^2} \right] K_{H_{\delta^2}}^{*}$$

INTRODUCTION

The preparation of firing tables for the launching of 30mm T306 E10 shell from supersonic aircraft requires a knowledge of the bullet's Aerodynamic behavior at supersonic and subsonic speeds for forward and rearward fire.[1] In addition, tail turret firings, under certain conditions, lead to large initial yaws. Aerodynamic measurements for this shell at large yaws were made in the wind tunnel, and initial yaws of fifteen degrees were obtained in the Transonic Range. To obtain small yaw data at supersonic Mach number, firings were made in the Aerodynamics Range and measurements were made in the wind tunnel; to obtain sonic and subsonic small yaw data, the Aerodynamics Range alone was used. This report contains the results of the firings in both ranges and compares them with wind tunnel measurements. These data supersede Reference 2.

EXPERIMENTAL PROCEDURE

Forty-three rounds were fired in the Aerodynamics Range from a tube with a twist of one turn in 16.5 calibers of travel, covering a range of Mach numbers from 0.46 to 2.42. Plate 1 is a shadowgraph of the shell at Mach number 2.2; and Plate 2, a photograph of the shell.

Early comparison of the yaw damping moment coefficient with that obtained from the wind tunnel showed disagreement. It was conjectured that the presence of the arming ball rotor in the fuze of the shell changed the damping properties of the shell in flight. Seven rounds with the arming ball rotor removed from the fuze were fired in the Aerodynamics Range at Mach numbers 1.8 and 2.1; these rounds verified the conjecture. The cavity obtained by removing the arming ball rotor was inert loaded to preserve the inertial properties of the shell In spite of this precaution there was a slight change in these properties which are given in Plate 3. Five rounds (two with the arming ball rotor removed) were fired in the Transonic Range from a gun tube which was notched at the muzzle in an attempt to obtain large yaw.

The firing of such a small projectile in the Transonic Range presented, at that time, a problem in triggering the stations. The standard

procedure for obtaining shadowgraphs in the Transonic Range[3] was as follows. A magnetic charge was put on the shell. Then, as the shell passed through solenoid coils, one for each station, the spark would fire after a pre-set time delay.

Because the firings of the 30mm T306 shell in the Transonic Range were planned as very-large-yaw firings, the expected trajectories could only have been accommodated by large solenoid coils. The required diameter for these coils would have been too large, relative to the size of the shell, for successful station triggering.

The solution to this dilemma was to use printed circuits (Plate 4). The printed circuit consisted of a sheet of paper upon which a continuous, rectilinear line was drawn with silver paint. The line traversed the width of the paper, returned to the other side at a level less than 3/4" below the first line, and continued crossing back and forth across the sheet with this same spacing. The shell, being 30mm (1.171") in diameter, was physically unable to pierce the sheet without establishing contact with the circuit. This breaking of the circuit, with a pre-set time delay, triggered the spark.

Since these firings, the Transonic Range has been equipped with photo-electric cells for triggering the stations. These cells worked successfully with large yaw firings of the 20mm T282E1 shell.

Even with a notched barrel the largest yaw obtained was only 15 degrees at the muzzle, and this damped to 8 1/2 degrees at mid-range.

EXPERIMENTAL RESULTS

A. Static Properties

1. Drag

The $K_{D_{range}}$ value for each round is determined by means of a cubic polynomial fit to time-distance measurements. Values for K_{D_0} and $K_{D_{\delta^2}}$ are obtained by plotting $K_{D_{range}}$ values vs mean squared yaw:

$$K_{D_{range}} = K_{D_0} + K_{D_{\delta^2}} \overline{\delta^2}$$

The accuracy of these determinations depends not only on the accuracy of the drag data, which are known to be very good, but also upon the spread of yaws obtained. Unfortunately, the rounds fired in the Aerodynamics Range reached average yaw levels of only three degrees. Since $K_{D_{\delta^2}}$ was well determined in the Wind Tunnel[4] for supersonic Mach numbers, those values were used for determining K_{D_0} by means of the above relationship. The larger yaw rounds fired in the Transonic Range traversed a sufficient amount of printed circuit paper within the timing stations to increase the drag of the shell noticeably. Otherwise, those rounds would have provided the necessary yaw spread for a good determination of K_{D_0} and $K_{D_{\delta^2}}$ without resorting to Wind Tunnel data.

Sonic and subsonic data were reduced to zero yaw by standard techniques. Figure 1 is a plot of the resulting K_{D_0} vs Mach number. Wind tunnel values fall slightly below range values. It should be noted that the wind tunnel tested a model of the shell whereas range firings were done with actual production rounds.

A Q function was computed for rounds in the region $1.4 < M < 2.5$:

$$Q = \sqrt{1 + M^2 K_{D_0}} = a + bM$$

$$a = .8353 \pm .0035 \text{ s. d.}$$

$$b = .2649 \pm .0019 \text{ s. d.}$$

2. Lift

The variation of the lift force with angle of attack is linear up to about six degrees. Since almost all the firings in this report have yaw levels below six degrees, $K_{L_{range}} = K_{L_0}$. Only one round (No. 2-3151), which has the largest root mean squared yaw of 8 1/2°, has a $K_{L_{range}}$ significantly greater than K_{L_0}. From wind tunnel measurements[4] $K_{L_{\delta^2}} = 2.5$ at $M = 2$. $K_{L_{range}}$ for Rd. No. 2-3151, when handled in the same manner set forth in Reference 5 agrees with the wind tunnel results.

K_{L_0} vs M is given in Figure 2. The rising and dipping of the curve which occur through the transonic region was substantiated by using a reduction which allows $K_{L_{range}}$ to vary with Mach number[6]. Computed dK_{L}/dM slopes are shown in Figure 2 as short lines, and the dashed curve represents the trend through this region.

Assuming K_{L_0} constant with Mach number in the region $1.4 < M < 2.5$, K_{L_0} has a standard deviation of 3.5% about a value of .924. Wind tunnel measurements show slightly higher values for K_{L_0} than those obtained in the range.

3. Overturning moment and center of pressure of normal force

The removal of the arming ball rotor from the fuze resulted in a rearward shift of the center of mass of .074 caliber. The $K_{M_{range}}$ values plotted in Figure 3 have been corrected to the c.m. position of the shell with the arming ball rotor in the fuze. For these firings, because of the linearity of the overturning moment with angle of yaw in the yaw region concerned, $K_{M_{range}} = K_{M_0}$. The wind tunnel values[4] for K_{M_0} fall slightly below those of the range at higher Mach numbers. The center of pressure of the normal force, CP_N, is plotted vs Mach number in Figure 4.

B. Dynamic Properties

Certain aerodynamic forces and moments of this projectile are so strongly nonlinear with yaw that this nonlinearity cannot be neglected. In Reference (5) there have been derived the necessary yaw parameters against which the measured aerodynamic coefficients should graph linearly. For cubic variations with yaw of the Magnus moment and yaw damping moment the following equations arise:

$$(1)\quad (K_H - K_{MA})_{range} = K_{H_0} - K_{MA_0} + K_{H_{\delta^2}}^{*} \left[\frac{\phi_1' K_{20}^2 - \phi_2' K_{10}^2}{\phi_1' - \phi_2'}\right] - \frac{k_2^2}{k_1^2}\left[\frac{\phi_1' + \phi_2'}{\phi_1' - \phi_2'}\right]\left[K_{10}^2 - K_{20}^2\right] \quad K_{T_{\delta^2}}^{*}$$

$$(2)\quad K_{T_{range}} = K_{T_0} + K^{*}_{T_{\delta}2}\ \delta_e^{\,2} + \frac{k_1^{\,2}}{k_2^{\,2}} \left[\frac{\phi_1'^{2} K_{10}^{\,2} - \phi_2'^{2} K_{20}^{\,2}}{\phi_1'^{2} - \phi_2'^{2}}\right] K^{*}_{H_{\delta}2}$$

where the starred terms are defined by:

$$K^{*}_{H_{\delta}2} = K_{H_{\delta}2} - K_{MA_{\delta}2} + \frac{1}{2} K_{MA_0}$$

$$K^{*}_{T_{\delta}2} = K_{T_{\delta}2} - \frac{1}{2} K_{T_0} .$$

1. Magnus moment

It is known that the Magnus moment of a pure cylinder shows mild nonlinearity with yaw (7). This nonlinearity, though relatively stronger than that observed in other aerodynamic moments, is almost negligible for yaws up to five degrees. Therefore, when strong nonlinearity is evidenced for a conventional shell for yaws less than five degrees, ballisticians are bound to express concern. Such is the situation with the 30mm T306 E10 shell (Ref. 8).**

To handle the Magnus data of the rounds, it was assumed that the last term of Eq. (2) was negligible:

$$(4)\qquad \therefore K_{T_{range}} = K_{T_0} + K^{*}_{T_{\delta}2}\ \delta_e^{\,2}$$

A least squares fit for rounds where $\delta_e^{\,2} < .0042$ resulted in

$$K_{T_0} = .047 \pm .010 \text{ s.d.}$$

$$K^{*}_{T_{\delta}2} \doteq K_{T_{\delta}2} = -36 \pm 4 \text{ s.d.}$$

The very few larger yaw firings would provide radically different values indicating either higher order effects or a non-polynomial variation of k_T with δ.

**Investigations are being conducted in the wind tunnel and in the Aerodynamics Range to determine the causes of the strong nonlinearity, such as rotating band effect, variation of transition point, or particular shape of the base of this shell.

In Reference 5, C. H. Murphy suggests that when an aerodynamic moment requires more than a simple cubic to describe its functional relationship with δ, the range data be divided into two (or more) yaw groups. A least squares fit for a particular group will provide K_{T_0} and $K_{T_{\delta^2}}$ for that portion of the moment vs. δ curve corresponding to the yaw interval of that group.** To compare the range data with wind tunnel measurements, k_T vs. α can be computed via definition:

$$(5) \qquad \begin{cases} k_T = (K_{T_0} + K_{T_{\delta^2}} \; \delta^2) \; \delta \\ \delta^2 = \sin^2 \alpha \; . \end{cases}$$

In Figure 5 the range determination of k_T vs α for α between zero and three degrees is compared with wind tunnel measurements.

Where the firings are too few to determine K_{T_0} and $K_{T_{\delta^2}}$ for use in Eq. (5), such as the case of the four larger yaw rounds in this report, a somewhat different treatment can be made for comparison with wind tunnel measurements. In range firings k_T would be constant for circular yawing motion. The concept of effective squared yaw essentially implies that only one $K_{T_{range}}$ is associated with that class of angular motions for which $\delta_e{}^2$ is the same. Thus, $K_{T_{range}}$ can be associated with a circular yawing motion with amplitude arc sin $\sqrt{\delta_e{}^2}$.

$$\therefore (6) \qquad k_{T_{range}} = K_{T_{range}} \; \delta = (K_{T_0} + K^*_{T_{\delta^2}} \; \delta^2) \; \delta$$

where $\qquad \delta = \sqrt{\delta_e{}^2}$.

Hence, by means of Eqs. (4) and (6) ,

$$(7) \qquad \begin{cases} k_T = k_{T_{range}} + \frac{1}{2} K_{T_0} \; \delta^3 = (K_{T_{range}} + \frac{1}{2} \; K_{T_0} \; \delta^2) \; \delta \\ \alpha = \text{arc} \sin \delta \end{cases}$$

**In Reference 9, C. H. Murphy further presents a means of handling non-polynomial nonlinearities, such as k_T vs α in Figure 5. However, more data than those now available would be needed to apply this technique to the 30mm T306 shell.

where $\delta = \sqrt{\overline{\delta_e^2}}$.

Using the wind tunnel determination of K_{T_0} , a (k_T, α) value can be computed for each of the four larger yaw rounds by means of Eq. (7). (In this case however, the K_{T_0} term of Eq. (7) was negligible, i.e., $k_T \doteq K_{T_{range}} \delta$.) These four points are also plotted in Figure 5. Considering the highly nonlinear nature of k_T with δ, the agreement between the two measurement facilities is very encouraging.

At the risk of being redundant, Figure 6 is presented to show how wind tunnel measurements, when transformed into K_T vs δ^2, compare with range data. Various portions of the wind tunnel curve of Figure 5 were approximated by cubics, resulting in the K_T vs δ^2 curves of Figure 6. It is evident that extrapolations of such curves are not always valid.

K_{T_0} (i.e., K_T at $\alpha = 0$) vs. M is plotted in Figure 7.

2. Damping moment

Early comparison between the wind tunnel's $(K_{H_0} - K_{MA_0})$ and the Aerodynamics Range's $(K_H - K_{MA})_{range}$ showed serious disagreement. It was felt that the presence of the arming ball rotor in the fuze radically changed the damping properties of the shell in flight, and, hence, the computed $(K_H - K_{MA})_{range}$ was an adulterated term. To test this hypothesis, firings with the arming ball rotor removed were conducted in both ranges. The presence of the ball reduces the moment and the data shows much greater scatter. The scatter probably arises from individual idiosyncrasies of ball-shell interaction of each round. These phenomena increase with increasing Mach number.

Although the major discrepancy between the original range data and wind tunnel data can be attributed to the arming ball rotor, wind tunnel data still do not completely agree with range data obtained from the firings with the arming ball rotor removed. Figure 8 is a plot of $(K_H - K_{MA})$ vs. M and includes both range and wind tunnel data. The

"without-ball" firings at $M = 1.8$ agree with wind tunnel data; those at $M = 2.1$ are considerably larger than wind tunnel data. The $M = 2.1$ firings, however, have larger yaws than the $M = 1.8$ firings. It could be conjectured that the damping moment may be highly nonlinear with yaw around $M = 2.0$. (The observed Magnus nonlinearity, $K_{T_{\delta^2}}$, does not account for the difference since $K_{10} \doteq K_{20}$ (Eq. 1)). To bring the two measuring facilities into agreement would require $(K_{H_{\delta^2}} - K_{MA_{\delta^2}})$ to be of the order of 400; but wind tunnel measurements show a value of -8 for $(K_{H_{\delta^2}} - K_{MA_{\delta^2}})$ at $M = 2.0$. Since the Air Force has abandoned this shell, it is felt that additional range firings to clarify this discrepancy should not be made. Such nonlinearity investigations are being conducted on better experimental configurations and also on standard shell still in use.

3. Yaw Damping Rates and the Arming Ball Rotor Effect

Precessional

The precessional yaw damping rate, λ_2, primarily reflects the behavior of K_T. Consequently, λ_2 data are handled in the same manner as were $K_{T_{range}}$ data. λ_2 vs δ_{e2}^2 for the region $1.2 < M < 2.5$ is plotted in Figure 9. Based on Figure 9, λ_2 vs. M at zero yaw is plotted in Figure 10.

Nutational

Extensive investigations made (and still being made) into the dynamic* effects of the arming ball rotor on the flight of the 20mm HEI, T282E1 shell showed that the nutational yaw damping rate, λ_1, is decreased in proportion to the frequency $\dot{\phi}_1$ provided that the angular velocity of the shell, ω, is large enough to arm the fuze:

$$\dot{\phi}_1 = \frac{A\omega}{2B} \quad (1 + \sigma)$$

where ω is fixed by the muzzle velocity and gun twist and where only σ varies with the density of air. For the 30mm T306 E10 shell, 57,000 rpm are required to arm the fuze. Since the firings in this program were made from a gun with a twist of 1:16.5, those rounds above $M = 1.4$ are the only

*Excluding the effect produced by the inherent change in the physical properties.

ones believed to have armed the fuze and, hence, produce a decrease in λ_1 (Fig. 11). If the shell were still to be used from high speed aircraft flying at altitudes between 30 and 60 thousand feet, standard firing conditions (gun twist of 1:25 and muzzle velocity of 2700 fps) would produce nutational frequencies between 12,400 and 12,800 rpm. In the firings of this report (1:16.5 twist), such nutational frequencies were produced at M = 1.6. Thus, the ball effect for the anticipated firing conditions would be a reduction in λ_1 measurements (as determined by the aerodynamic forces and moments alone, i.e., "without-ball") of about 0.0025 $(ft)^{-1}$ regardless of the speed of the aircraft.

Since the discrepancies in the damping moment date from the wind tunnel and from the "without-ball" firings cannot at present, be resolved, a search into the ball effect on λ_1 of the data in this report appears futile. Should this projectile again be considered for Air Force use, then further firings could be made to resolve the discrepancies and to investigate the ball effect. It is hoped that the thorough investigation being conducted on the ball effect of the flight of the 20mm T282E1 shell would be completed by that time and that those results would facilitate any further 30mm T306 E10 investigation.

4. Stability

The shell is dynamically unstable below a Mach number one. Moreover, this instability cannot be overcome by resorting to higher spin(10). However, it has been observed that for the 105mm M1 shell(11), for example, there exists a "trim"* angle of yaw such that the shell is dynamically stable at yaws above "trim". Such a trim angle may exist for the 30mm T306 E10 shell in subsonic flight. The rounds in this report presumably have average yawing levels below "trim" and, consequently, have dynamic instability.

Eugene T. Roecker — EUGENE T. ROECKER

Eugene D. Boyer — EUGENE D. BOYER

*The word "trim" is borrowed from the field of aeronautics to designate a limit cycle yawing motion.

REFERENCES

1. Poor, C. L. "The Flight Mechanics of Spinning Shell at Large Angles of Initial Yaw," BRL TN 1038, August 1955.

2. Boyer, Eugene, D. "Aerodynamics of the 30mm Shell HE T306 E10," BRL TN 896, May 1954.

3. Rogers, Walter, K. "The Transonic Free Flight Range," BRL Report 849, February 1953.

4. Buford, William, E. "Aerodynamic Characteristics of the 30mm Shell T306 E10," BRL TN 1019, July 1955.

5. Murphy, C. H. "The Measurement of Non-Linear Forces and Moments by Means of Free Flight Tests," BRL Report 974, February, 1956.

6. Murphy, C. H. "Data Reduction for the Free Flight Spark Ranges, BRL Report 900, February 1954.

7. Buford, William E. "Magnus Effect in the Case of Rotating Cylinders and Shell," BRLM 821, July 1954.

8. Platou, A. S., and Sternberg, J. "The Magnus Characteristics of a 30mm Aircraft Bullet," BRL Report 994, September 1956.

9. Murphy, C. H. "Prediction of the Motion of Missiles Acted on by Non-Linear Forces and Moments," BRL Report 995, October, 1956.

10. Murphy, C. H. "On the Stability Criteria of the Kelley-McShane Linearized Theory of Yawing Motion," BRL Report 853, April 1953.

11. Roecker, Eugene, T. "The Aerodynamic Properties of the 105-mm Shell, M1, in Subsonic and Transonic Flight," BRLM 929, September 1955.

12. Boyer, Eugene, D. "Aerodynamic Characteristics for Small Yaws of 20mm Shell, HEI, T282E1 with Fuze M505 for Mach numbers .36 to 3.78, BRLM 916, August 1955.

13. Buford, William, E. "Aerodynamic Characteristics of 20mm Shell T282E1. HEI," BRLM 834, October 1954.

14. Roecker, Eugene, T. "Large Yaw Firings of the 20mm, HEI, T282E1 Shell with Fuze T196, at Mach Number 2.3," BRLM 888, April 1955.

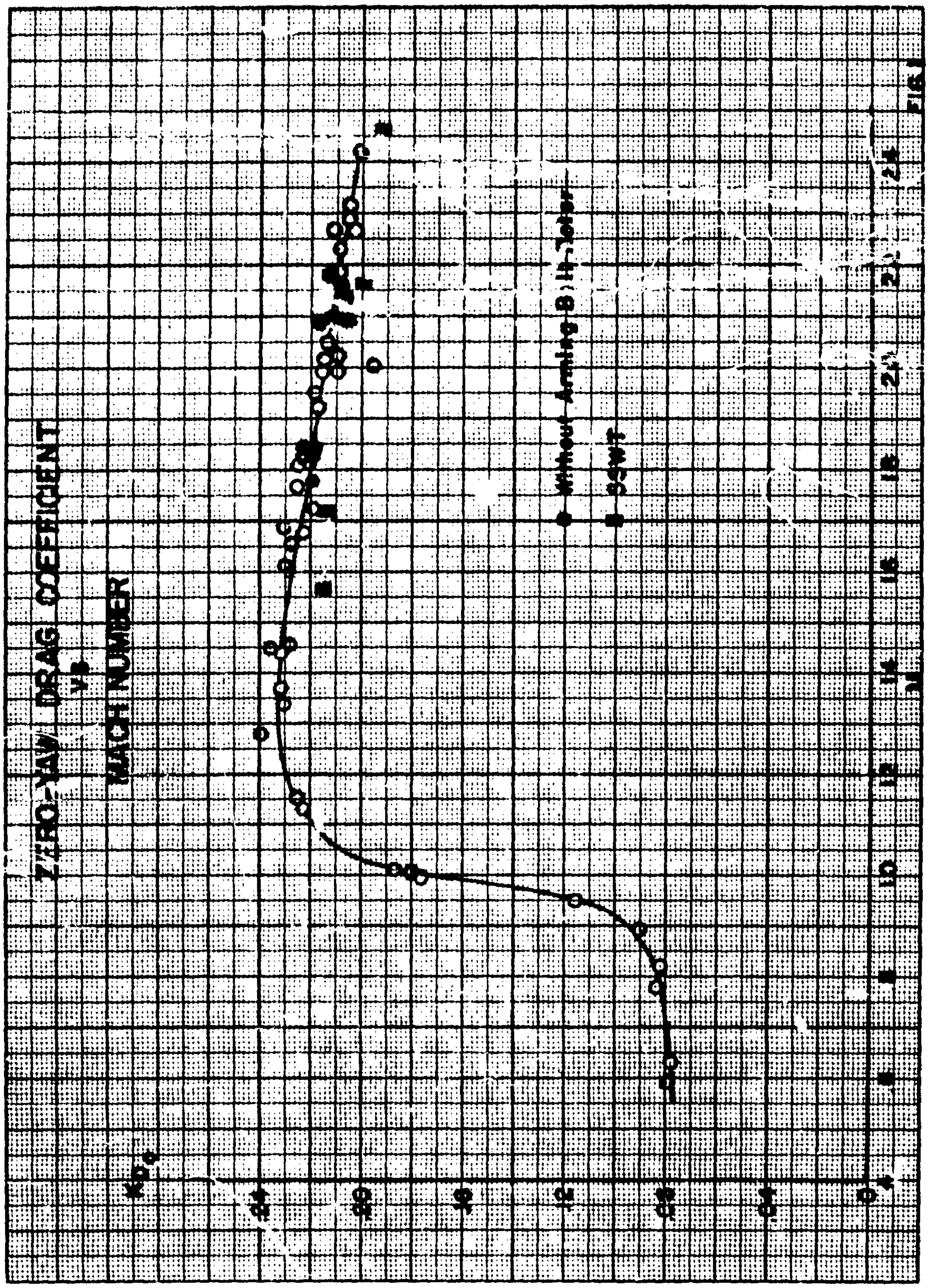
ZERO-YAW DRAG COEFFICIENT
VS
MACH NUMBER
M
FIG 1

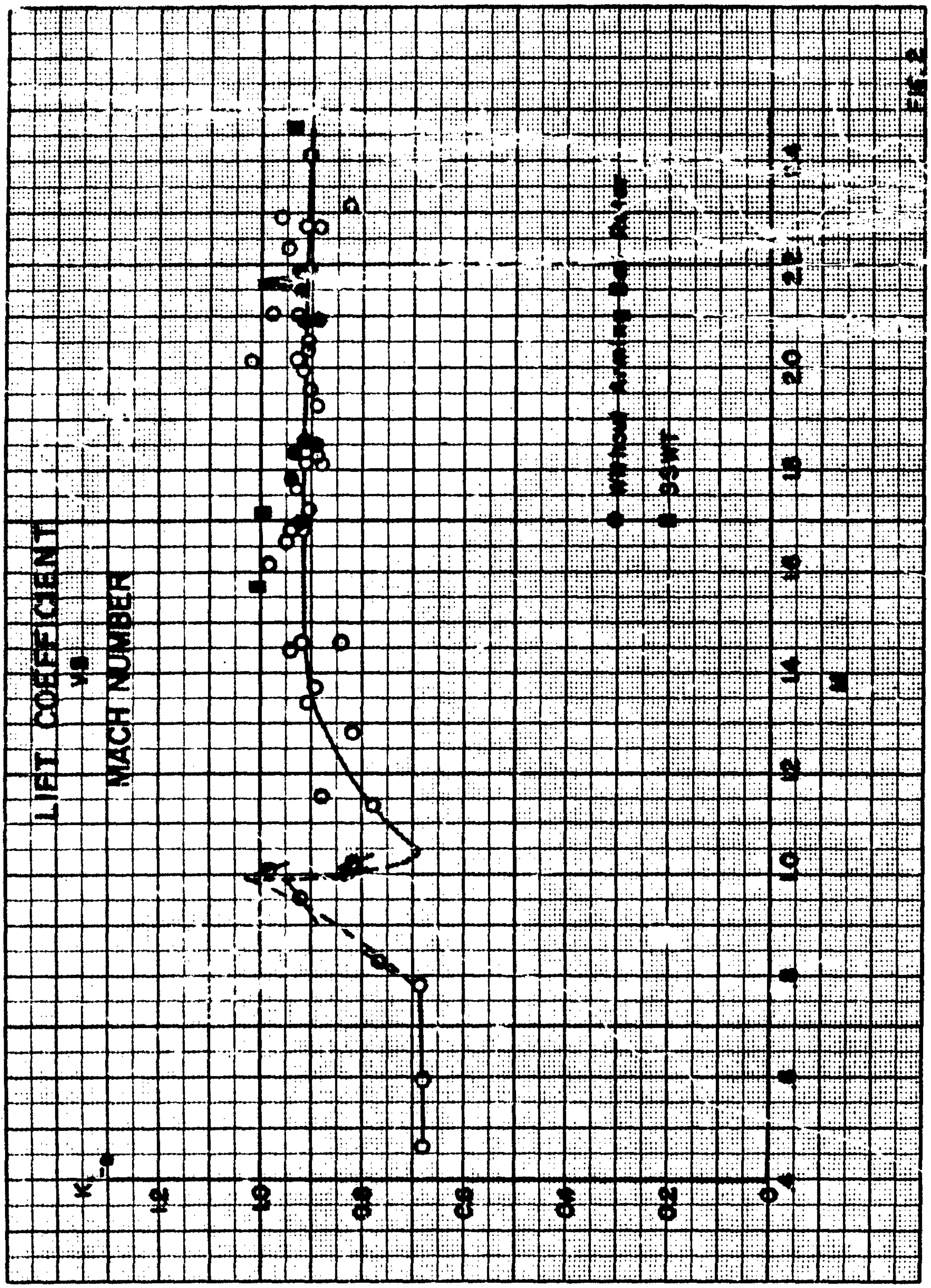
LIFT COEFFICIENT
vs
MACH NUMBER
1.2
1.0
0.8
0.6
0.4
0.2
0
.4
.6
.8
1.0
1.2
1.4
1.6
1.8
2.0
2.2
2.4
M

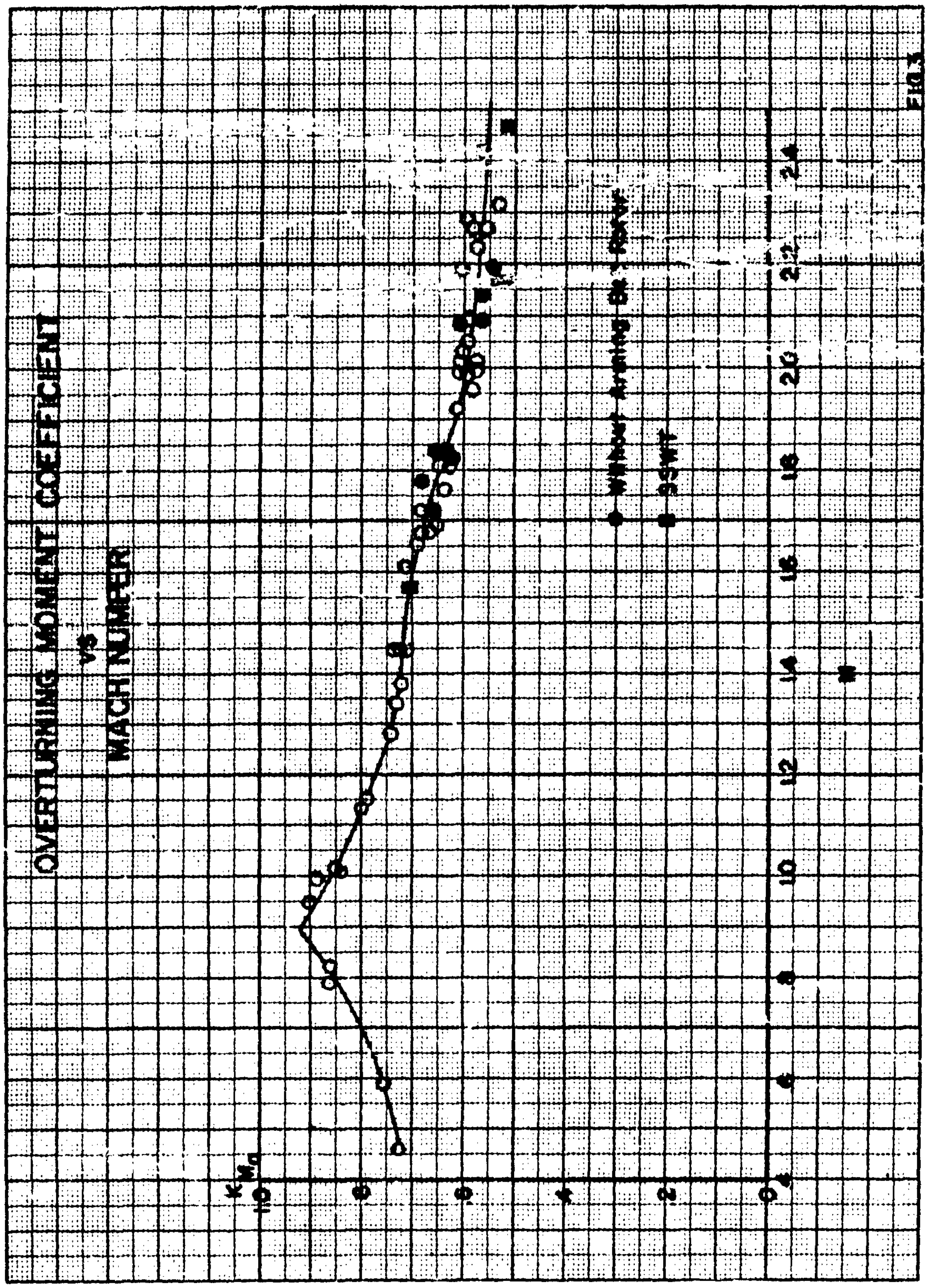
OVERTURNING MOMENT COEFFICIENT
VS
MACH NUMBER
K_{M_α}
10
8
6
4
2
0
.4
.6
.8
1.0
1.2
1.4
1.6
1.8
2.0
2.2
2.4
M

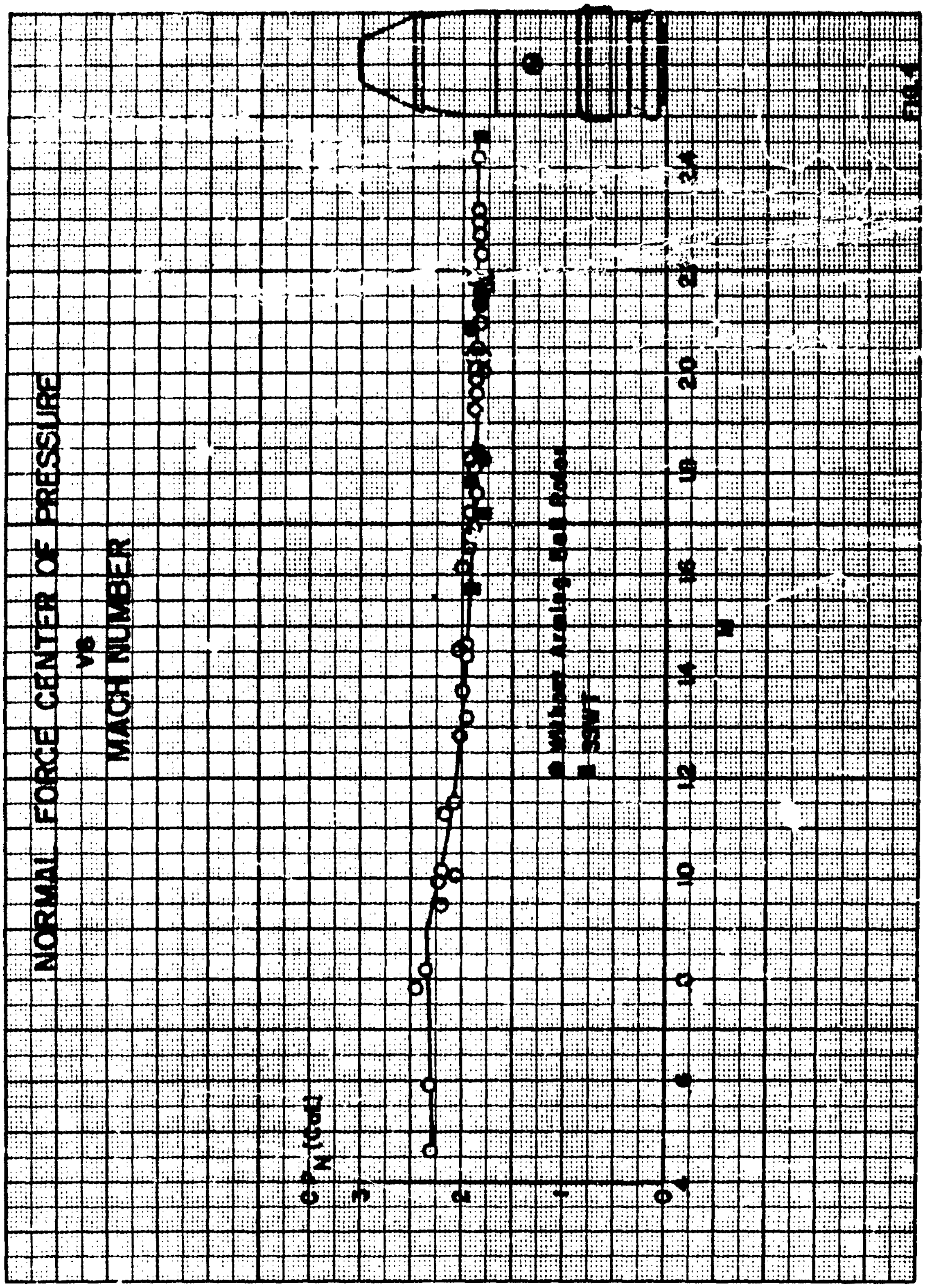
NORMAL FORCE CENTER OF PRESSURE
VS
MACH NUMBER
M
0
1
2
3
4
6
8
10
12
14
16
18
20
22
24

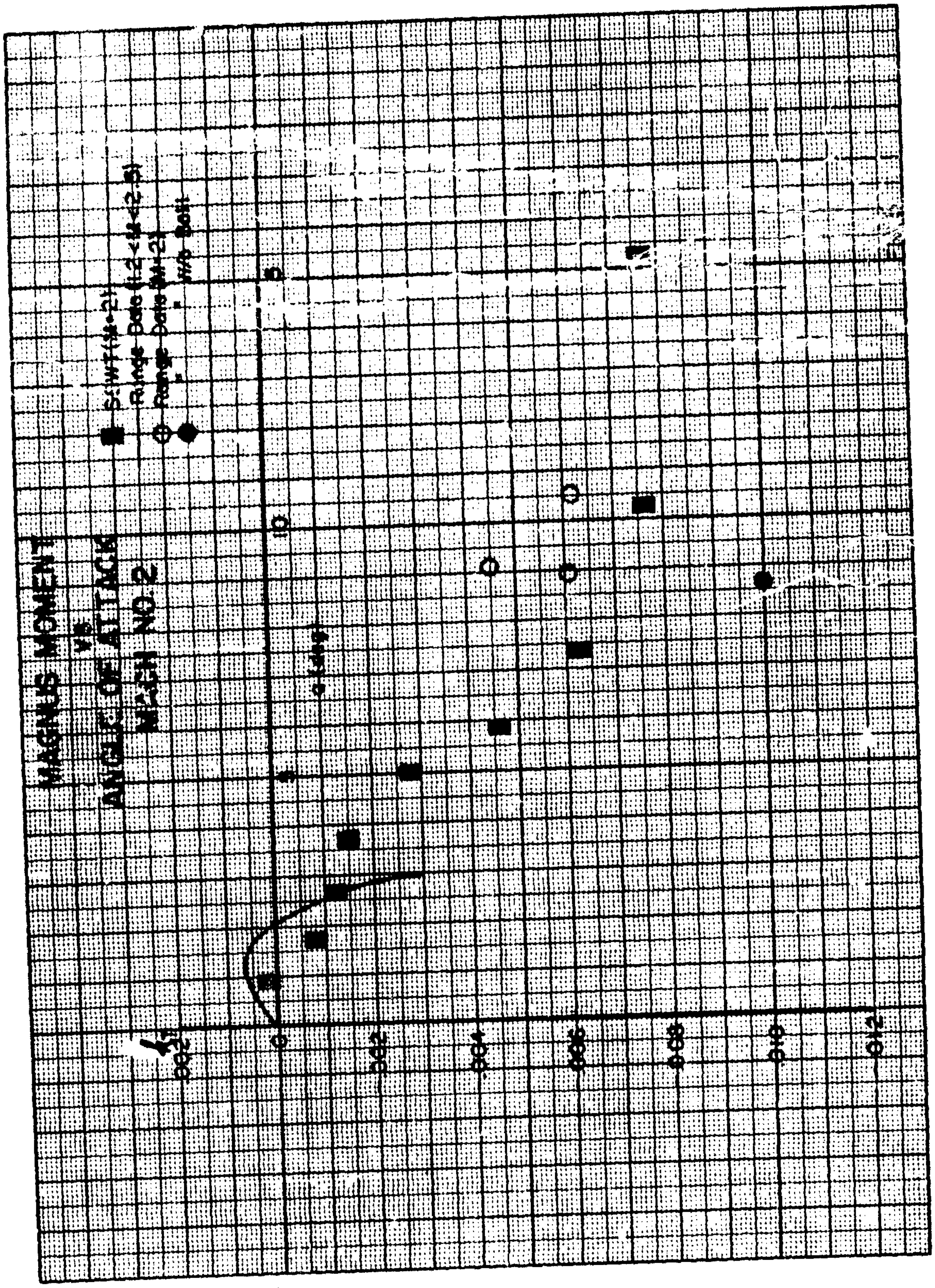
MAGNUS MOMENT
VS
ANGLE OF ATTACK
MACH NO 2
-0.02
0
0.02
0.04
0.06
0.08
0.10
0.12
5
10

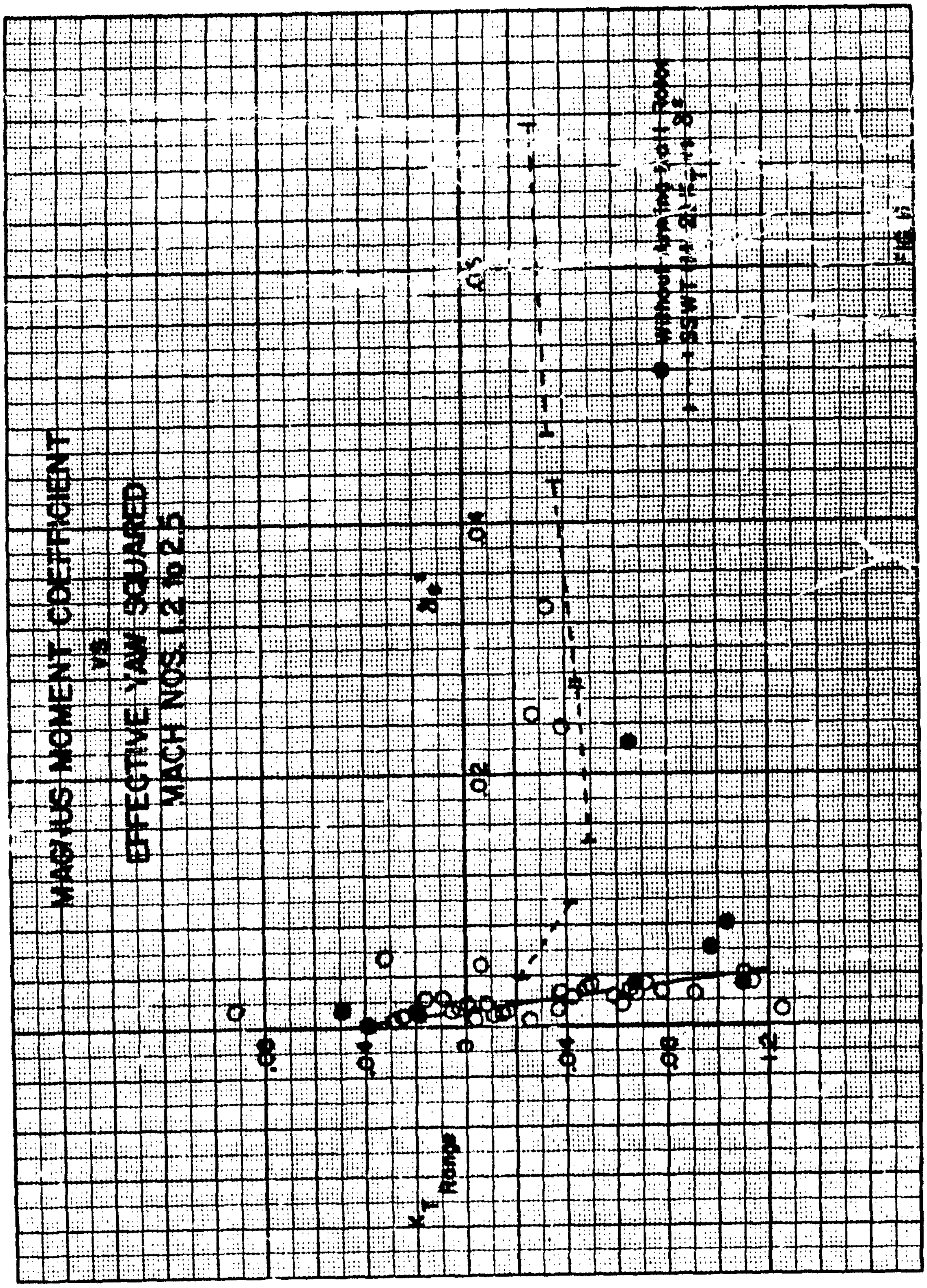
MAGNUS MOMENT COEFFICIENT
vs
EFFECTIVE YAW SQUARED
MACH NOS 1.2 to 2.5

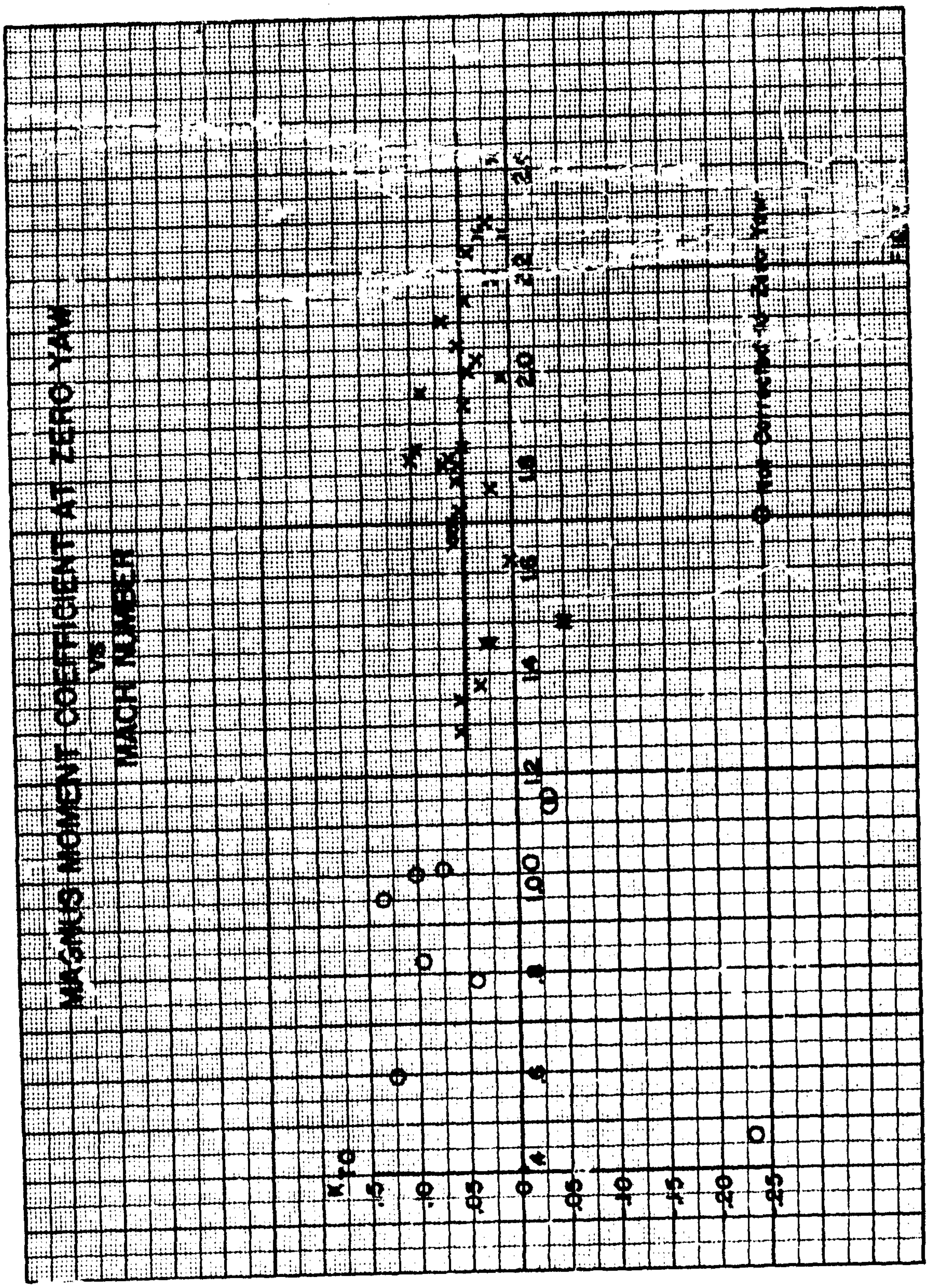
MAGNUS MOMENT COEFFICIENT AT ZERO YAW
VS
MACH NUMBER
O Not Corrected to Zero Yaw

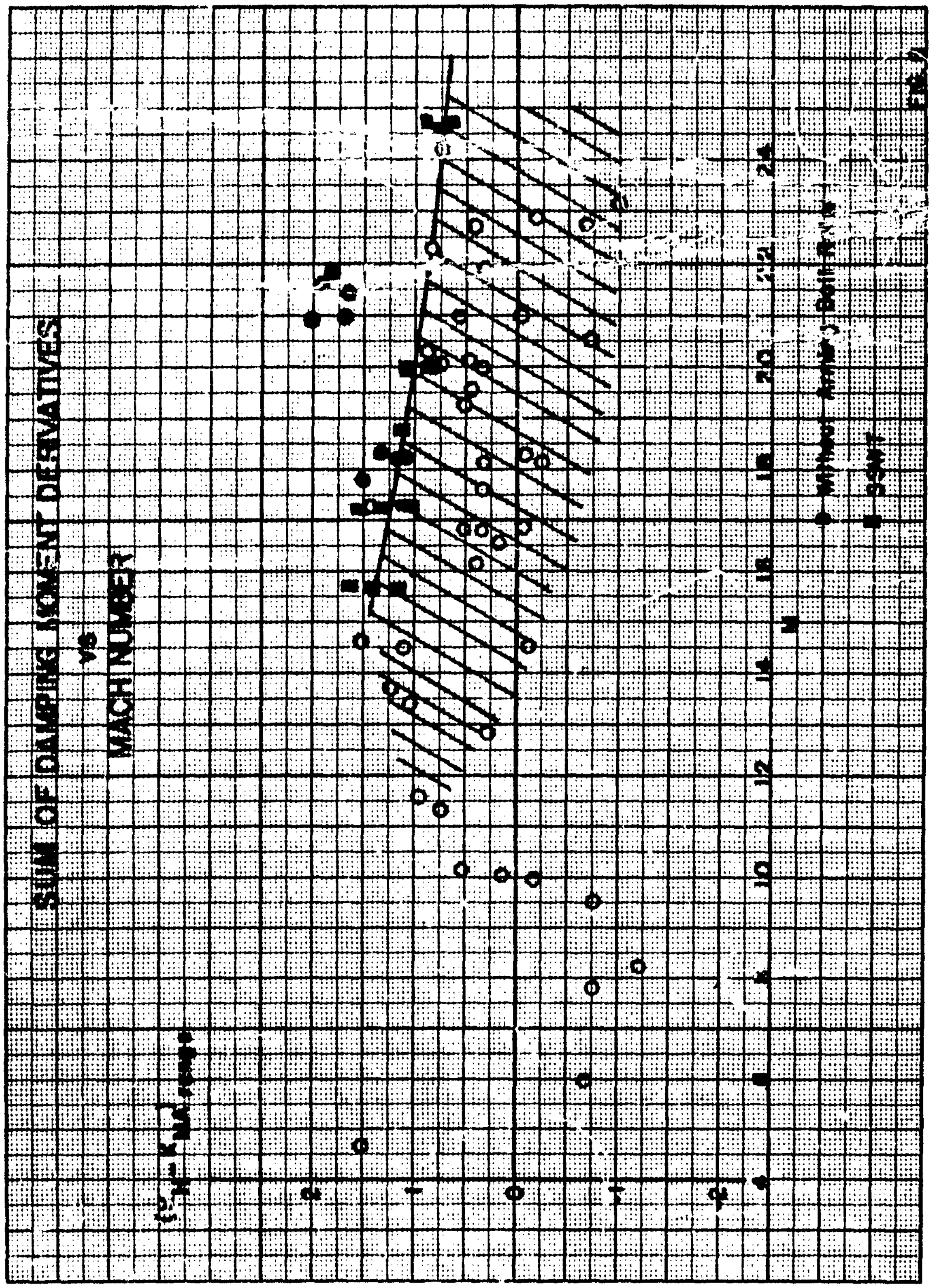
SUM OF DAMPING MOMENT DERIVATIVES
VS
MACH NUMBER

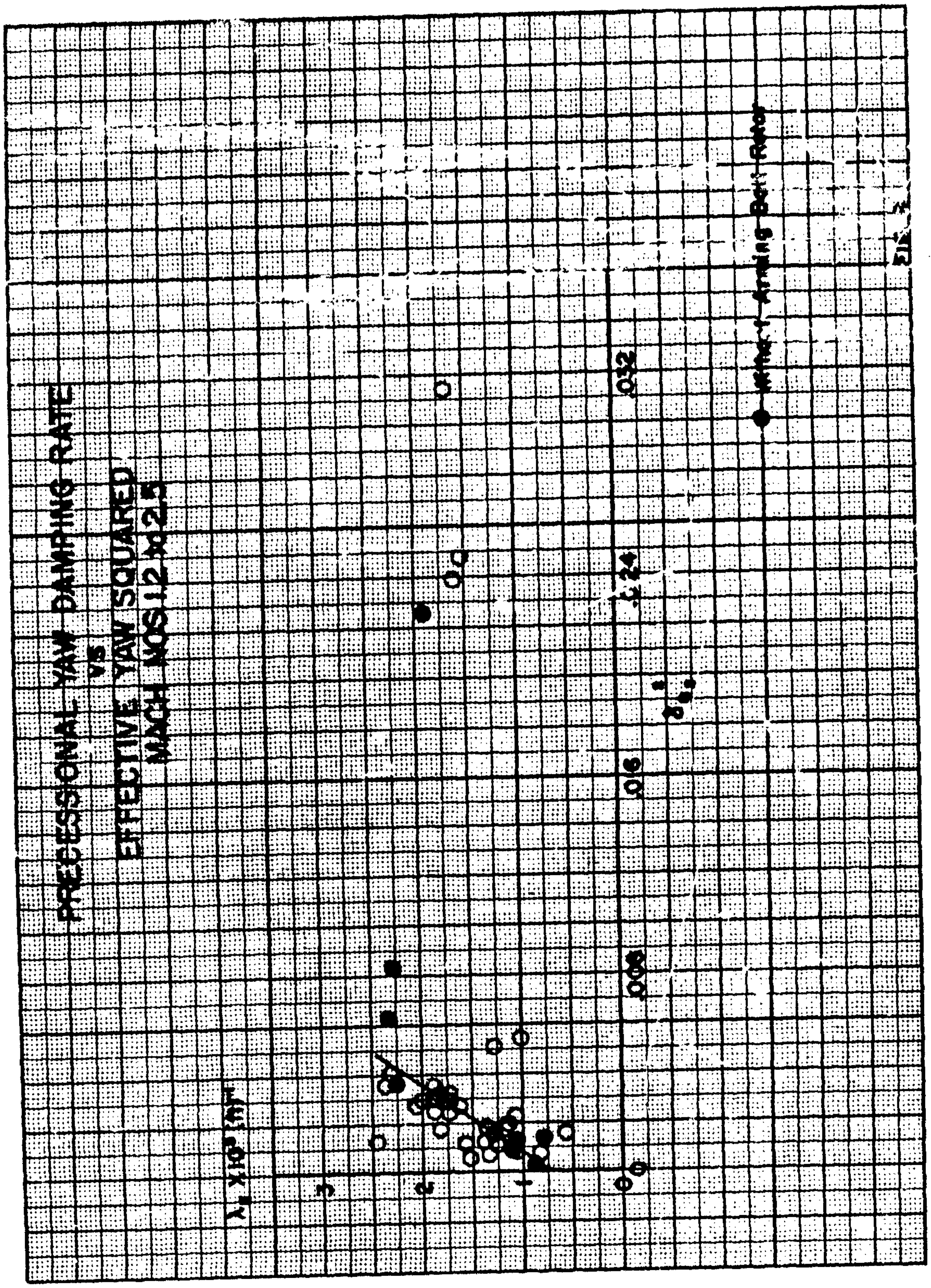
PRECESSIONAL YAW DAMPING RATE
VS
EFFECTIVE YAW SQUARED
MACH NOS 1.2 - 2.5
.008
.016
.024
.032
1
2
3

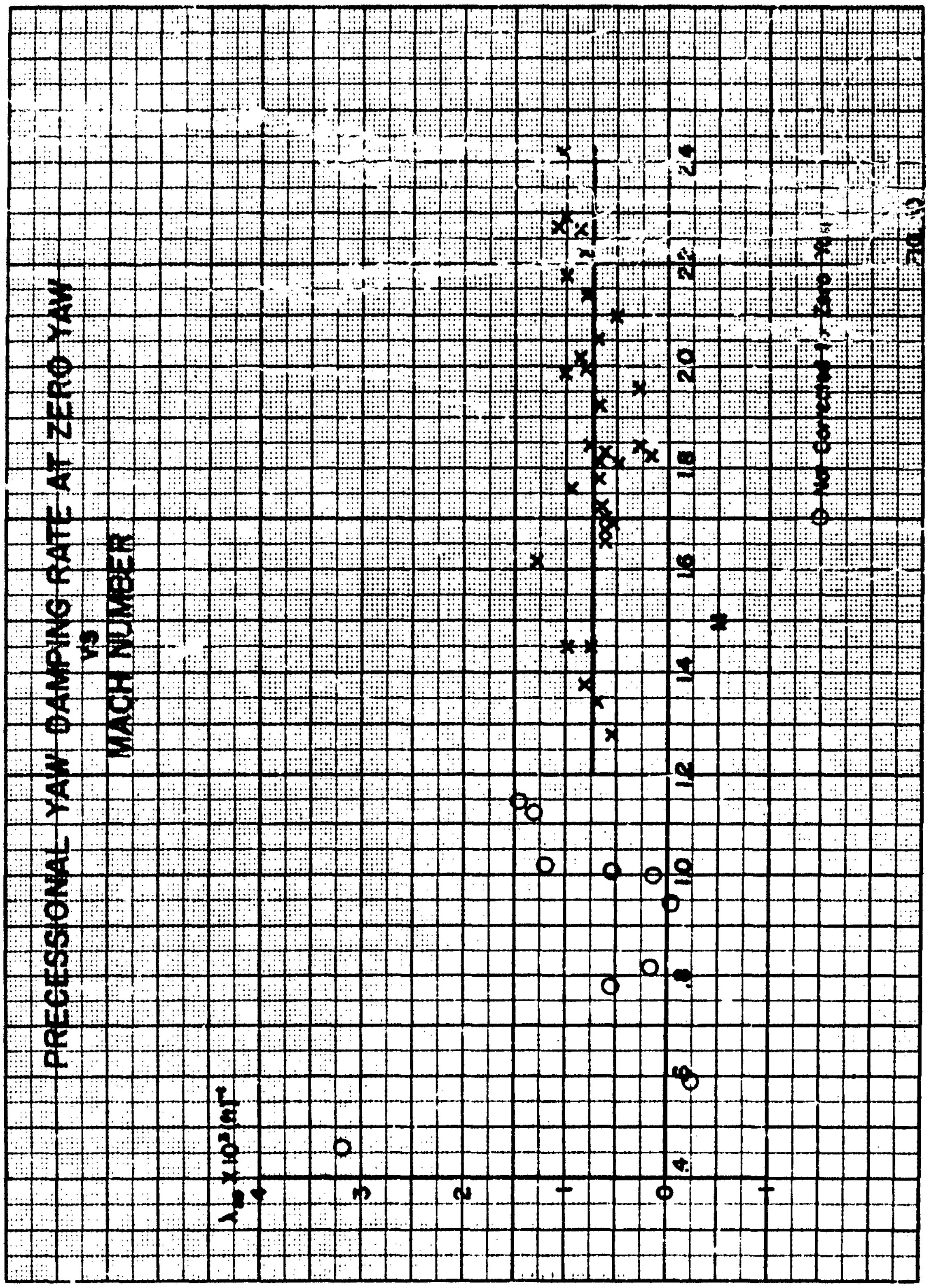
PRECESSIONAL YAW DAMPING RATE AT ZERO YAW
VS
MACH NUMBER
4
3
2
1
0
.4
.6
.8
1.0
1.2
1.4
1.6
1.8
2.0
2.2
2.4

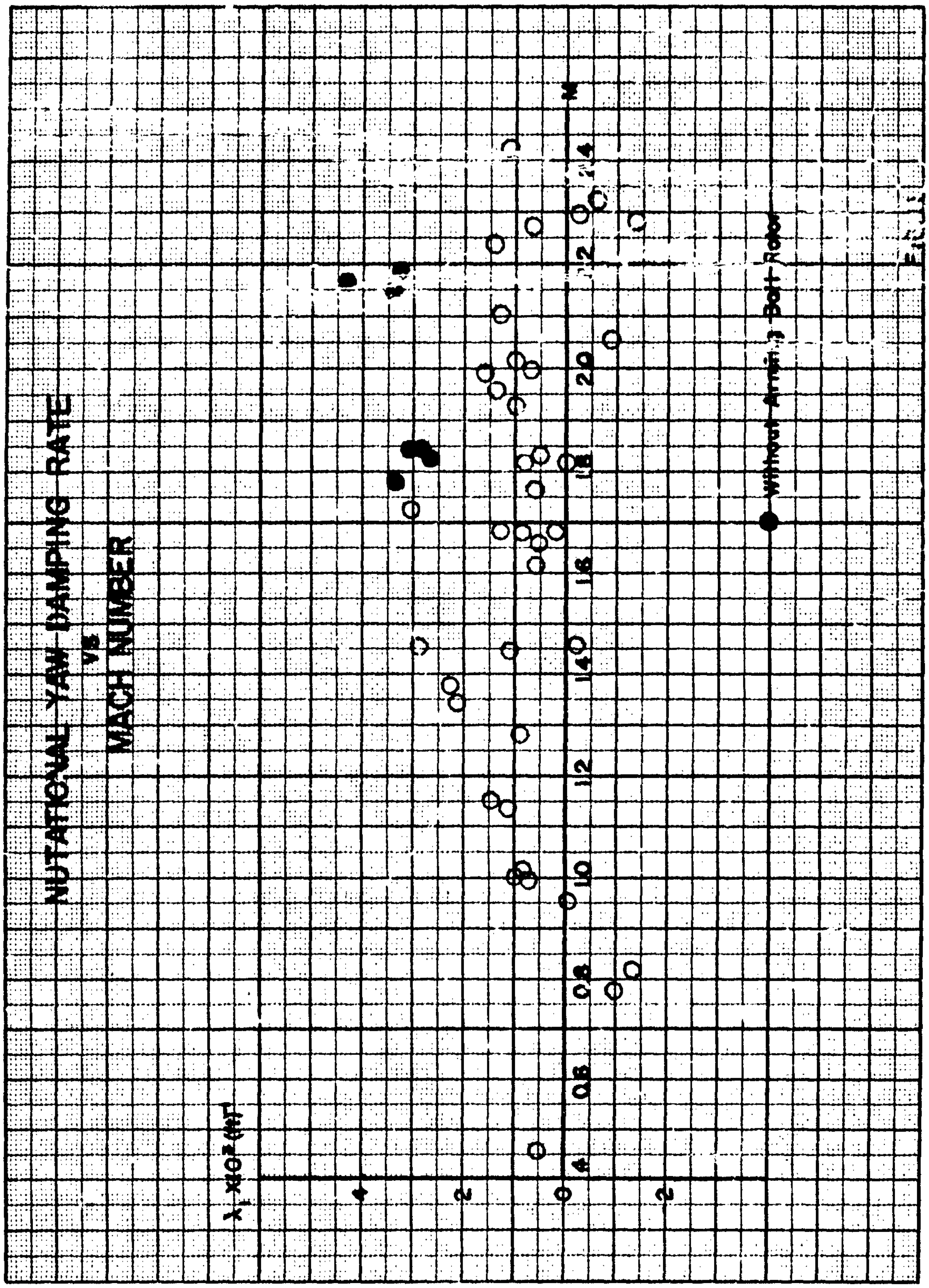
NUTATIONAL YAW DAMPING RATE
vs
MACH NUMBER
$\lambda_1 \times 10^2$ (ft^{-1})
4
2
0
2
.4
0.6
0.8
1.0
1.2
1.4
1.6
1.8
2.0
2.2
2.4
M

APPENDICES

Appendix A Tables of Data

The aerodynamic data for each round is given in the following tables:

Table I: Aerodynamic Range Firings with Arming Ball Rotor, M = .46 to M = 1.72.

Table II: Aerodynamic Range Firings with Arming Ball Rotor, M = 1.76 to M = 2.42

Table III: Transonic Range Firings with Arming Ball Rotor, M = 2

Table IV: Aerodynamic Range Firings without Arming Ball Rotor, M = 1.77 to M = 2.18

Table V: Transonic Range Firings without Arming Ball Rotor, M = 2

TABLE Ia

AERODYNAMICS RANGE FIRINGS WITH ARMING BALL ROTOR

Round No.	M	$\overline{\delta^2} \times 10^2$	K_{D_r}	K_{M_r}	K_{L_r}	$(K_H - K_{MA})_r$	K_{T_r}	$\lambda_1 \times 10^3$ $(ft)^{-1}$	$\lambda_2 \times 10^3$ $(ft)^{-1}$	ϕ_1' (deg/ft)	ϕ_2' (deg/ft)
1-3333	.463	.360		.724	.68	1.50	-.236	.41	3.18	36.38	1.22
3334	.593	.255	.0834	.757	.68	-.71	.123	-.17	-.26	38.59	1.19
3332	.636	.098	.0786								
3329	.783	.209	.0879	.860	.69	-.78	.042	-1.07	.56	38.87	1.33
3330	.823	.144	.0847	.856	.77	-1.21	.096	-1.35	.16	38.59	1.33
3348	.894	.046	.0913								
3347	.951	.236	.1258	.900	.92	-.75	.136	-.10	-.05	39.14	1.36
3327	1.003	.050	.1786	.885	.83	-.18	.099	.60	.15	40.00	1.34
3346	1.007	.139	.1844	.836	.98	.13	.074	.89	.56	39.73	1.24
3328	1.017	.095	.1909	.847	.81	.52	-.012	.79	1.19	39.61	1.29
3323	1.133	.110	.2286	.793	.78	.73	-.032	.98	1.32	40.69	1.17
3322	1.152	.155	.2324	.785	.88	.91	-.032	1.33	1.45	39.98	1.19
3606	1.282	.051	.2422	.740	.81	.25	.026	.66	.82	39.98	1.10
3320	1.339	.242	.2419	.728	.91	1.08	-.071	1.28	1.38	40.63	1.09
3335	1.374	.156	.2392	.719	.89	1.22	-.059	1.62	1.70	40.19	1.07
3319	1.447	.093	.2356	.714	.94	1.09	-.126	.73	2.[illegible]1	42.32	1.01
3608	1.454	.095	.2399	.727	.84	1.49	-.019	2.50	1.23	40.50	1.08
3318	1.455	.064	.2323	.740	.92	-.17	-.016	-.49	1.37	42.23	1.04
3609	1.614	.041	.2328	.714	.98	.39	-.026	.42	1.52	41.90	1.02
3336	1.655	.162	.2345	.688	.95	.14	-.039	-.17	1.60	41.56	.98
3326	1.677	.179	.2311	.665	.92	.34	-.049	.12	1.68	42.16	.96
3325	1.679	.148	.2298	.578	.94	.50	-.009	.80	1.33	43.17	.95
3547	1.691	.079	.2353	.651	.93	-.11	-.001	-.26	1.25	41.24	.94
3324	1.724	.134	.2227	.682	.91	1.42	.005	2.65	1.12	41.33	1.01

Subscript r refers to coefficients as measured in the range, on the basis of linearized theory.

TABLE Ib

AERODYNAMICS RANGE FIRINGS WITH ARMING BALL ROTOR

Round No.	M	$\delta_e^2 \times 10^2$	K_{10}	K_{20}	$\bar{s}$	s*	N	N_T	ϵ_Y	ϵ_3	S_L
1-3333	.463	.711	.058	.016	1.7	4.6	15	3	.0023	.0038	.42
3334	.593	.421	.039	.034	1.2	4.4	27	7	.0018	.0094	.78
3332	.636							7			
3329	.783	.364	.038	.027	-1.9	3.9	23	8	.0017	.0068	.56
3330	.823	.230	.030	.022	-1.7	3.9	29	9	.0026	.0152	.56
3348	.894							7			
3347	.951	.354	.037	.028	.7	3.7	31	8	.0015	.0250	.74
3327	1.003	.074	.016	.015	.4	3.8	30	8	.002[illegible]	.0157	.33
3346	1.007	.214	.028	.024	.8	4.0	30	8	.0023	.0440	.02
3328	1.017	.148	.024	.018	1.2	4.0	29	8	.0015	.0276	.50
3323	1.133	.166	.025	.020	1.1	4.2	31	8	.0017	.0071	.63
3322	1.152	.238	.031	.021	1.0	4.3	31	9	.0019	.0118	.75
3606	1.282	.082	.018	.013	1.1	4.5	27	9	.0022	.0087	.42
3320	1.339	.350	.036	.030	1.2	4.6	27	8	.0024	.0123	1.28
3335	1.374	.259	.029	.026	1.0	4.7	25	6	.0012	.0055	1.05
3319	1.447	.142	.023	.019	1.5	4.7	28	9	.0025	.0132	.91
3608	1.454	.137	.022	.020	.7	4.6	27	9	.0021	.0060	.75
3318	1.455	.111	.021	.015	3.1	4.5	27	9	.0018	.0775	.61
360[illegible]	1.614	.066	.016	.012	1.6	4.7	26	8	.0019	.0095	.58
3336	1.655	.281	.034	.022	2.2	4.9	31	9	.0018	.0093	1.12
3326	1.677	.309	.035	.025	1.8	5.0	30	9	.0024	.0083	1.25
3325	1.679	.202	.028	.021	1.2	4.9	26	7	.0015	.0120	1.18
3547	1.691	.173	.027	.016	2.5	5.1	23	7	.0016	.0079	.85
3324	1.724	.132	.027	.024	.6	4.9	16	5	.0020	.007[illegible]	1.09

*The gyroscopic stability factor has been converted from the 1-16.5 gun twist of the firings to the standard 1-25 twist.

TABLE IIa

AERODYNAMICS RANGE FIRINGS WITH ARMING BALL ROTOR

Round No.	M	$\overline{\delta^2}$x10^2	K_{D_r}	K_{M_r}	K_{L_r}	$(K_H-K_{MA})_r$	K_{T_r}	λ_1x10^3 $(ft)^{-1}$	λ_2x10^3 $(ft)^{-1}$	ϕ_1' (deg/ft)	ϕ_2' (deg/ft)
1-3549	1.761	.103	.2298	.636	.93	.34	-.037	.19	1.57	41.96	.91
3550	1.811	.161	.2280	.626	.91	.33	-.042	.14	1.60	41.66	.90
3548	1.813	.111	.2293	.642	.88	-.25	.003	-.48	1.1[illegible]	41.90	.92
3607	1.825	.148	.2283	.631	.89	-.10	.016	-.08	1.03	42.[illegible]7	.90
3610	1.926	.192	.2246	.611	.89	.52	-.066	.26	1.7[illegible]	42.0[illegible]	.87
3613	1.954	.148	.2225	.581	.90	.44	.009	.83	1.08	41.55	.84
3338	1.990	.176	.2210	.593	.92	.99	-.092	.87	2.05	42.55	.84
3340	1.996	.182	.2226	.607	.92	.34	-.068	-.07	1.88	42.95	.86
3341	2.014	.079	.2168	.604	.93	.45	-.013	.65	1.35	42.94	.85
3339	2.051	.052	.2159	.592	.91	-.72	.022	-1.14	1.02	42.74	.83
3555	2.100	.211	.2194	.592	.93	.55	-.052	.45	1.70	40.27	.88
3337	2.102	.347	.2216	.587	.98	-.07	.032	.13	.99	41.53	.83
3556	2.190	.325	.2197	.601	.91	.32	-.007	.47	1.24	40.54	.88
3342	2.232	.258	.2175	.575	.95	.84	-.111	.43	2.26	42.11	.81
3615	2.272	.108	.2142	.556	.89	-.69	-.063	-1.91	1.78	42.39	.79
3560	2.272	.191	.2094	.582	.91	.41	-.078	-.07	1.95	39.79	.89
3344	2.293	.045	.2072	.592	.96	-.22	-.004	-.49	1.32	42.41	.83
3561	2.315	.099	.2080	.525	.83	-1.00	.091	-1.07	.54	40.79	.79
3343	2.421	.218	.2065	.563	.90	.74	-.114	.22	2.30	41.21	.82

TABLE IIb

AERODYNAMICS RANGE FIRINGS WITH ARMING BALL ROTOR

Round No.	M	$\delta_e^2 x10^2$	K_{10}	K_{20}	$\bar{s}$	s*	N	N_T	ϵ_Y	ϵ_S	S_L
1-3549	1.761	.168	.026	.018	1.7	5.3	31	9	.0011	.0052	1.06
3550	1.811	.263	.032	.024	1.8	5.3	30	9	.0013	.0058	1.37
3548	1.813	.183	.027	.019	3.4	5.2	26	6	.0018	.0111	1.00
3607	1.825	.242	.031	.022	2.1	5.3	28	9	.0025	.0078	1.34
3610	1.926	.318	.036	.024	1.7	5.5	29	9	.0022	.0084	1.47
3613	1.954	.231	.029	.025	1.1	5.8	15	6	.0021	.0054	1.61
3338	1.990	.286	.033	.026	1.4	5.6	22	5	.0021	.0115	1.71
3340	1.996	.304	.035	.024	2.0	5.5	30	9	.0017	[illegible]	1.58
3341	2.014	.130	.022	.018	1.3	5.5	28	7	.0017	.0063	1.16
3339	2.051	.095	.020	.012	-13.5	5.7	28	8	.0017	.0073	.72
3555	2.100	.343	.037	.026	1.6	5.7	29	9	.0013	.0070	1.60
3337	2.102	.551	.045	.038	1.7	5.7	19	6	.0027	.0056	2.65
3556	2.190	.518	.044	.036	1.4	5.6	15	4	.0030	.0069	2.14
3342	2.232	.416	.041	.028	1.7	5.8	25	6	.0022	.0144	2.19
3615	2.272	.192	.029	.015	-23.2	6.0	22	9	.0026	.0078	1.06
3560	2.272	.305	.034	.027	2.0	5.8	16	5	.0017	.0046	1.58
3344	2.293	.080	.018	.012	3.1	5.7	30	7	.0025	.0121	.83
3561	2.315	.162	.025	.019	-.6	6.4	18	5	.0019	.0057	1.29
3343	2.421	.359	.037	.029	1.8	5.9	19	5	.0020	.0082	1.78

*The gyroscopic stability factor has been converted from the 1-16.5 twist of the firings to the standard 1-25 twist.

TABLE IIIa

TRANSONIC RANGE FIRINGS WITH ARMING BALL ROTOR

Round No.	M	$\overline{\delta^2}$x10^2	K_{D_r}	K_{M_r}	K_{L_r}	$(K_H-K_{MA})_r$	K_{T_r}	λ_1x10^3 (ft)$^{-1}$	λ_2x10^3 (ft)$^{-1}$	ϕ_1' (deg/ft)	ϕ_2' (deg/ft)
2-3153	2.000	1.708	.2641	.574	.93	.96	-.028	1.43	1.49	40.87	.85
3151	2.008	2.191	.2688	.573	1.02	.75	-.033	.98	1.64	41.02	.84
3150	2.029	1.607	.2602	.601	.91	.85	-.039	1.11	1.56	41.04	.88

TABLE IIIb

TRANSONIC RANGE FIRINGS WITH ARMING BALL ROTOR

Round No.	M	δ_e^2x10^2	K_{10}	K_{20}	$\bar{s}$	s*	N	N_T	ϵ_Y	ϵ_N	S_L
2-3153	2.000	2.490	.095	.082	1.0	5.8	13	8	.0059	.0110	.[illegible]7
3151	2.008	3.350	.109	.099	1.2	5.8	13	7	.0083	.0110	.65
3150	2.029	2.391	.092	.084	1.2	5.6	14	9	.0065	.0100	.43

*The gyroscopic stability factor has been converted from the 1-16.5 gun twist of the firings to the standard 1-25 twist.

TABLE IVa

AERODYNAMIC RANGE FIRINGS WITHOUT ARMING BALL ROTOR

Round No.	M	$\overline{\delta^2} \times 10^2$	K_{D_r}	K_{M_r}	K_{L_r}	$(K_H-K_{MA})_r$	K_{T_r}	$\lambda_1 \times 10^3$ $(ft)^{-1}$	$\lambda_2 \times 10^3$ $(ft)^{-1}$	ϕ_1' (deg/ft)	ϕ_2' (deg/ft)
1-3553	1.778	.074	.2228	.765	.94	1.49	.017	3.06	1.10	44.71	1.12
3554	1.832	.094	.2234	.712	.93	1.15	.018	2.39	1.09	45.56	1.01
3552	1.840	.092	.2223	.714	.90	1.05	.049	2.48	.75	44.15	1.06
3551	1.844	.019	.2238	.737	.91	1.32	.037	2.92	.87	46.03	1.05
3559	2.143	.242	.2147	.645	.92	1.65	-.069	2.56	1.92	42.92	.99
3558	2.161	.424	.2234	.618	.96	1.91	-.098	2.81	2.28	43.59	.94
3557	2.183	.225	.2192	.622	.92	1.82	-.113	2.38	2.29	43.14	.92

TABLE IVb

AERODYNAMIC RANGE FIRINGS WITHOUT ARMING BALL ROTOR

Round No.	M	$\delta_e^2 \times 10^2$	K_{10}	K_{20}	$\bar{s}$	s*	N	N_T	ϵ_Y	ϵ_S	S_L
1-3553	1.778	.113	.020	.018	.5	4.7	16	4	.0016	.005[illegible]	.75
3554	1.832	.128	.020	.022	.6	5.1	27	9	.0024	.0089	1.15
3552	1.840	.137	.022	.020	.5	5.1	20	6	.0021	.0070	.90
3551	1.844	.023	.008	.011	.5	4.9	27	9	.0015	.0056	.49
3559	2.143	.320	.033	.032	.9	5.6	24	8	.0023	.0072	1.70
3558	2.161	.636	.047	.044	.9	5.9	15	4	.0019	.0070	2.63
3557	2.183	.365	.037	.030	1.0	5.8	19	5	.0019	.0075	1.71

*The gyroscopic stability factor has been converted from the 1-16.5 gun twist of the firings to the standard 1-25 twist.

TABLE Va

TRANSONIC RANGE FIRINGS WITHOUT ARMING BALL ROTOR

Round No.	M	$\overline{\delta^2} \times 10^2$	K_{D_r}	K_{M_r}	K_{L_r}	$(K_H - K_{MA})_r$	K_{T_r}	$\lambda_1 \times 10^3$ $(ft)^{-1}$	$\lambda_2 \times 10^3$ $(ft)^{-1}$	ϕ_1' (deg/ft)	ϕ_2' (deg/ft)
2-3155	2.089	.392	.2366	.688	.89	2.00	-.105	2.87	2.24	42.27	1.06
3156	2.092	1.416	.2585	.647	.91	1.69	-.066	2.64	1.89	42.87	.98

TABLE Vb

TRANSONIC RANGE FIRINGS WITHOUT ARMING BALL ROTOR

Round No.	M	$\delta_e^2 \times 10^2$	K_{10}	K_{20}	$\bar{s}$	s*	N	N_T	ϵ_Y	ϵ_S	S_L
2-3155	2.089	.819	.047	.062	.9	5.1	14	9	.0079	.0120	.22
3156	2.092	2.261	.083	.094	.8	5.5	13	8	.0044	.0120	.39

*The gyroscopic stability factor has been converted from the 1-16.5 gun twist of the firings to the standard 1-25 twist.

APPENDIX B

PLATES

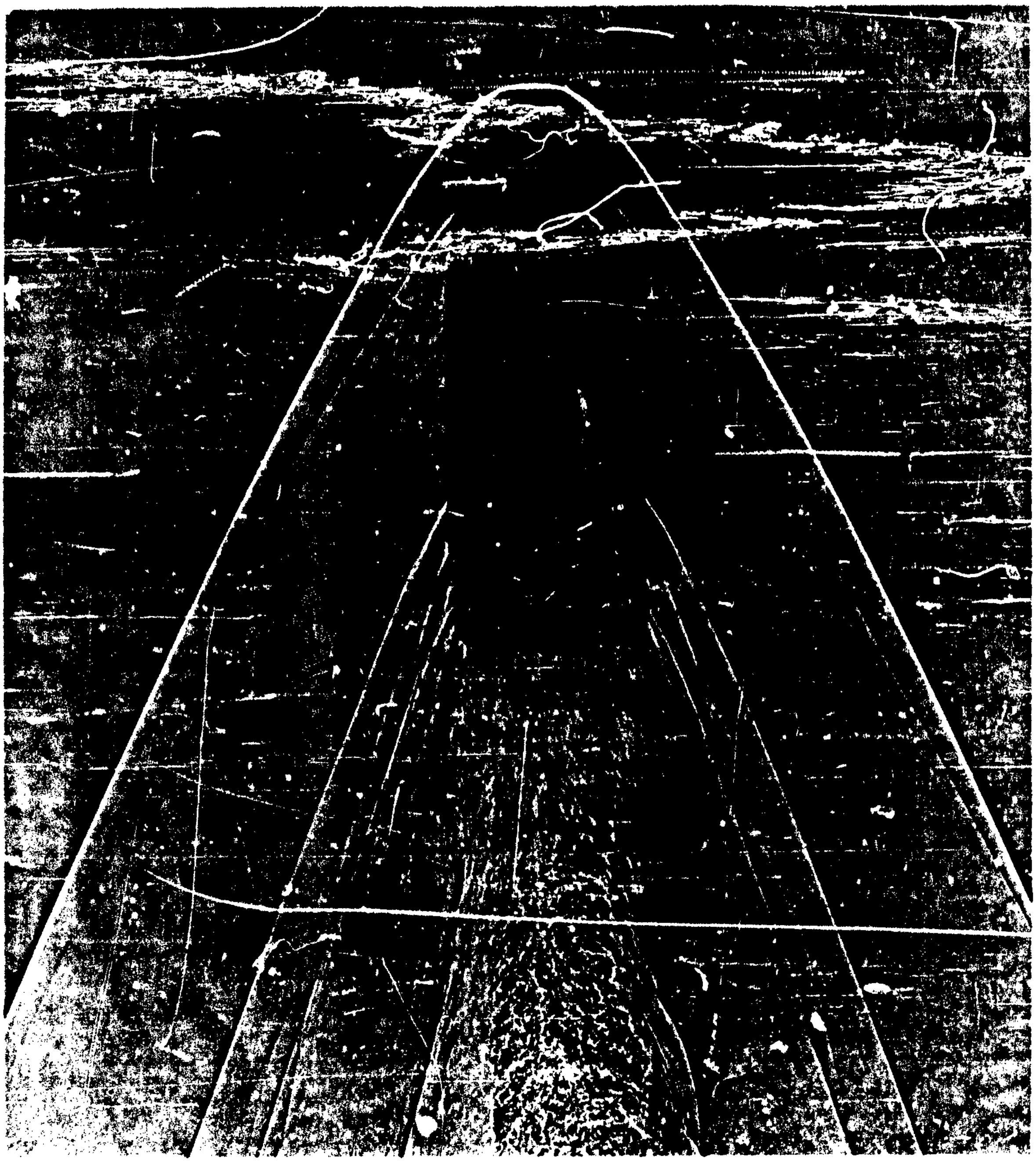

Plate 1: Shadowgraph of Shell $M = 2.2$

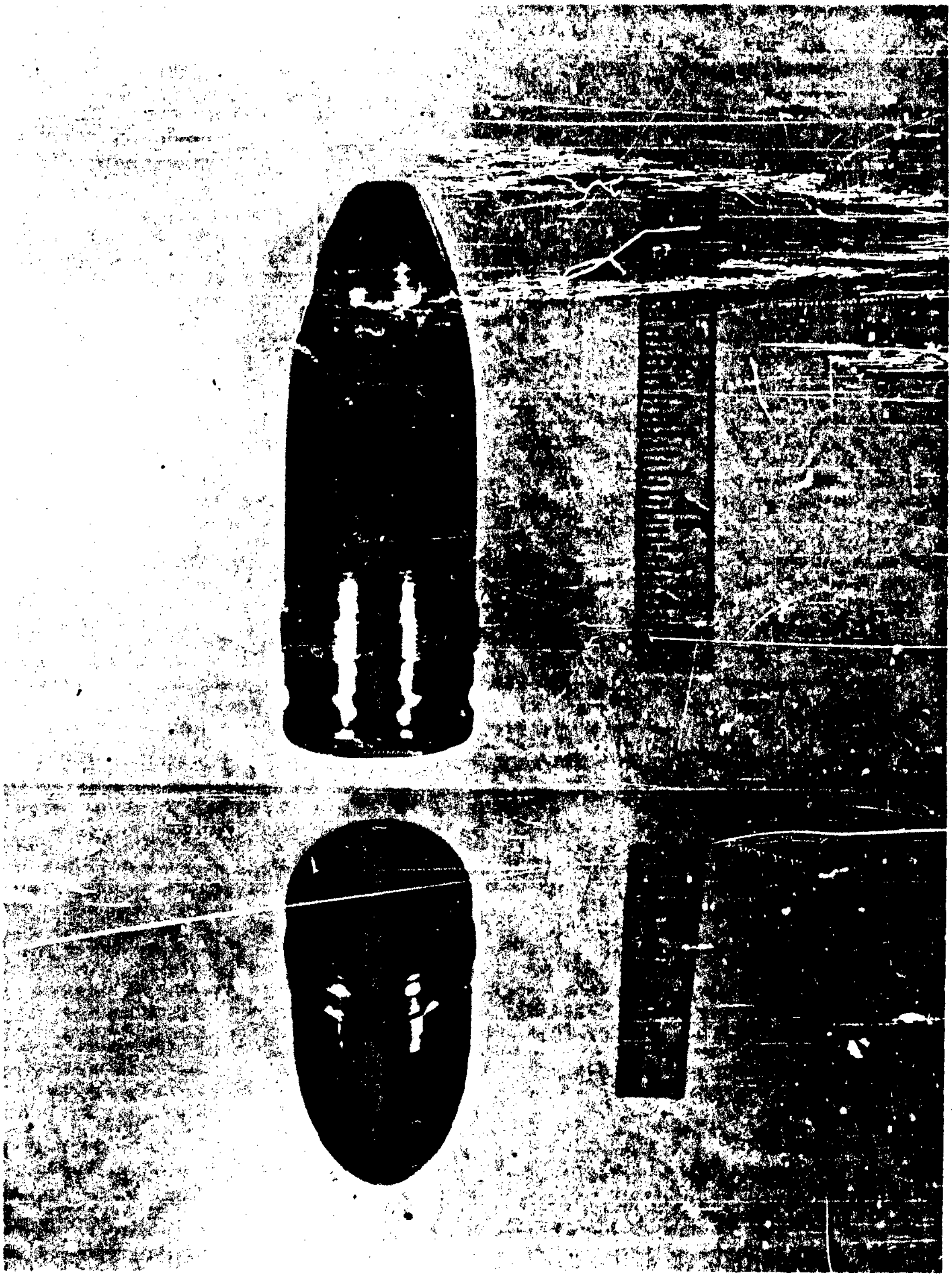

Plate 2: Photograph of Shell

30 MM HEI SHELL, T306E10

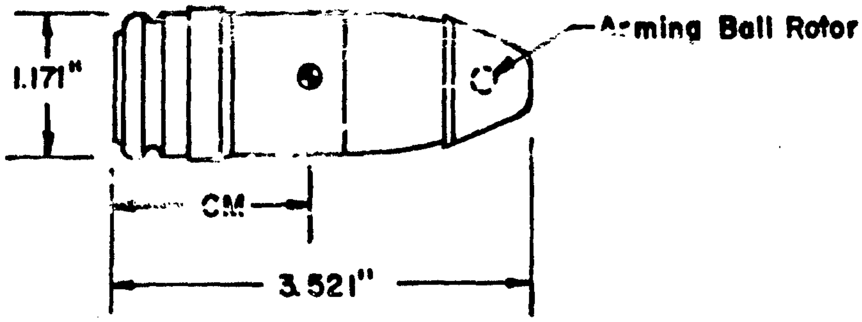

AERODYNAMICS RANGE SHELL			
T263 FUZE		MODIFIED T263 FUZE	
CM	1.564 in. = 1.336 Cal.	CM	1.478 in. = 1.262 Cal.
WT.	252.5 Grams	WT.	235.1 Grams
A	48.18 Gram-inches^2	A	47.26 Gram-inches^2
B	248.3 Gram-inches^2	B	229.5 Gram-inches^2

TRANSONIC RANGE SHELL			
T263 FUZE		MODIFIED T263 FUZE	
CM	1.560 in. = 1.332 CAL.	CM	1.502 in. = 1.283 CAL.
WT.	254.7 Grams	WT.	238.0 Grams
A	48.31 Gram-inches^2	A	47.76 Gram-inches^2
B	253.2 Gram-inches^2	B	235.5 Gram-inches^2

PLATE 3

Plate 4: Microflash of Shell

APPENDIX C

Extension of Data to Mach Number 3.2.

To obtain aerodynamic data at higher Mach numbers than those presented in the main body of the report, it was necessary to modify the standard 30-mm gun, with which only Mach numbers as large as 2.4 were achieved. The gun was modified by screwing a 37-mm chamber to the breech and adding a two-foot length of smoothbore 30-mm tube to the muzzle. These modifications increased the capabilities of the gun to a Mach number of 3.2.

Since the main body of this report was already written and the data analyzed, particularly the nonlinear Magnus moment, the data from the additional firings at M = 3.2 are presented here in appendix form. The data for five 30-mm T306 E10 rounds and for four rounds without the arming ball rotor in the fuze are given. For the most part these rounds have very small yaws and their data were considered to be too sketchy to give additional information on the dynamic problems discussed in the report.

Tables VI and VII list the aerodynamic data. Figure 12 consists of plots of the pertinent Figures (variation with Mach number only) from the main body of the report with the curves extended to M = 3.2. The only points plotted in Figure 12 are those obtained from the additional firings. K_T and λ_2 are not plotted since the highly nonlinear Magnus moment as evaluated in the main body of the report may not be applicable at M = 3. (Wind Tunnel measurements for Magnus do not go beyond M = 2.47.)

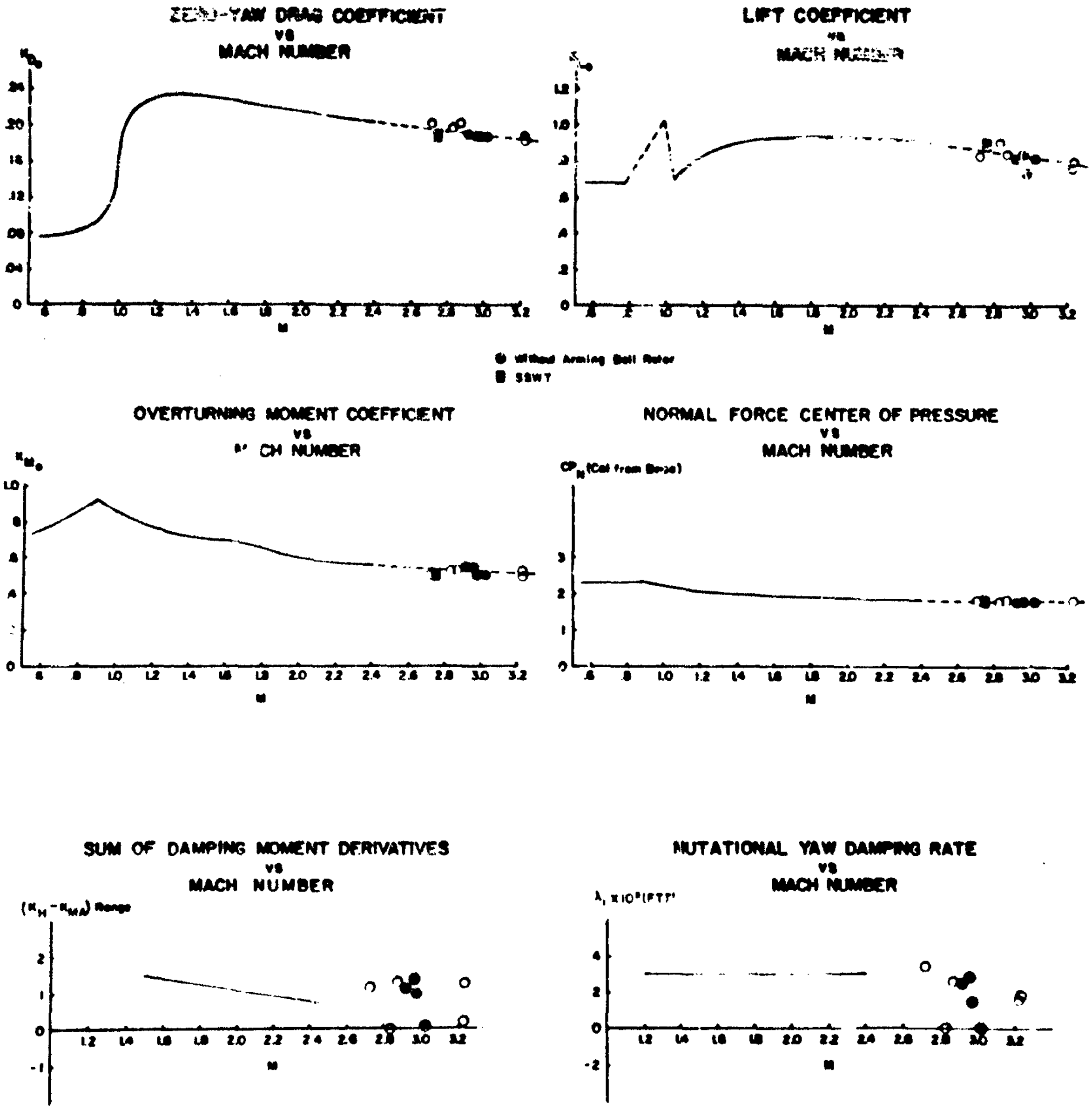
ZERO-YAW DRAG COEFFICIENT
VS
MACH NUMBER
LIFT COEFFICIENT
VS
MACH NUMBER
Without Arming Ball Rotor
SSWT
OVERTURNING MOMENT COEFFICIENT
VS
MACH NUMBER
NORMAL FORCE CENTER OF PRESSURE
VS
MACH NUMBER
SUM OF DAMPING MOMENT DERIVATIVES
VS
MACH NUMBER
NUTATIONAL YAW DAMPING RATE
VS
MACH NUMBER
M

FIGURE 12

TABLE VIa

AERODYNAMIC RANGE FIRINGS WITH ARMING BALL ROTOR*

Round No.	M	$\overline{\delta^2}$x10^2	K_{D_r}	K_{M_r}	K_{L_r}	$(K_H - K_{MA})_r$	K_{T_r}	λ_1x10^3 $(ft)^{-1}$	λ_2x10^3 $(ft)^{-1}$	ϕ_1' (deg/ft)	ϕ_2' (deg/ft)
1-4402	2.716	.372	.2025	.502	.83	1.16	-.042	1.66	1.45	25.55	1.17
4358	2.833	.027	.1957	.534	.91	-.05	.005	-.12	1.20	29.70	1.09
4360	2.867	.250	.2010	.532	.84	1.27	-.064	1.63	1.68	29.21	1.08
4406	3.226	.035	.1854	.499	.78	.22	.109	1.45	-.05	26.05	1.15
4398	3.231	.036	.1830	.525	.79	1.23	-.062	1.61	1.68	26.27	1.20

TABLE VIb

AERODYNAMIC RANGE FIRINGS WITH ARMING BALL ROTOR*

Round No.	M	δ_e^2x10^2	K_{10}	K_{20}	$\bar{s}$	s	N	N_T	ϵ_Y	ϵ_S	S_L
1-4402	2.716	.595	.048	.036	.9	6.0	21	8	.0024	.0126	1.09
4358	2.833	.044	.013	.010	2.2	7.4	24	8	.0023	.0088	.41
4360	2.867	.301	.032	.031	1.0	7.2	14	5	.0019	.0058	1.12
4406	3.226	.060	.016	.009	.0	6.2	19	8	.0022	.0129	.27
4398	3.231	.062	.016	.010	1.0	6.0	19	9	.0001	.0154	.29

*All rounds fired from a tube with a twist of one turn in 22.5 calibers of travel.

CONFIDENTIAL

TABLE VIIa

AERODYNAMIC RANGE FIRINGS WITHOUT ARMING BALL ROTOR*

Round No.	M	$\overline{\delta^2} \times 10^2$	K_{D_r}	K_{M_r}	K_{L_r}	$(K_H - K_{MA})_r$	K_{T_r}	$\lambda_1 \times 10^3$ $(ft)^{-1}$	$\lambda_2 \times 10^3$ $(ft)^{-1}$	ϕ_1' (deg/ft)	ϕ_2' (deg/ft)
1-4363**	2.915	.156	.1909	.547	.82	1.08	-.035	1.75	1.45	25.97	1.36
4361	2.958	.065	.1873	.543	.84	1.43	-.025	2.51	[illegible]	30.25	1.14
4364**	2.969	.048	.1871	.495	.73	.92	-.061	1.17	[illegible]	23.39	1.39
4366**	3.020	.092	.1867	.498	.81	.01	-.044	-.53	1.59	22.12	1.36

TABLE VIIb

AERODYNAMIC RANGE FIRINGS WITHOUT ARMING BALL ROTOR*

Round No.	M	$\delta_e^2 \times 10^2$	K_{10}	K_{20}	$\bar{s}$	s	N	N_T	ϵ_Y	ϵ	[illegible]
1-4363**	2.915	.219	.026	.029	.9	5.3	22	7	.0014	.0104	.69
4361	2.958	.091	.016	.020	.7	7.1	16	4	.0019	.0116	[illegible]
4364**	2.969	.078	.017	.014	1.1	4.7	20	8	.0018	.0166	[illegible]
4366**	3.020	.124	.019	.023	2.8	4.6	22	9	.0014	.0106	[illegible]

*All rounds fired from a tube with a twist of one turn in 22.5 Calibers of travel.

**These rounds were fired through a magnetic yaw inducer to reduce the spin and consequently produce more yaw.

Contractors received this report THRU their appropriate contracting agencies.

DISTRIBUTION LIST

No. of Copies	Organization
[illegible]	Chief of Ordnance Department of the Army Washington 25, D. C. Attn: ORDTB - Bal Sec ORDTS
10	British Joint Services Mission 1800 K Street, N. W. Washington 6, D. C. Attn: Mr. John Izzard, Reports Officer
4	Canadian Army Staff 2450 Massachusetts Ave.,N.W. Washington 8, D. C.
4	Chief, Bureau of Ordnance Department of the Navy Washington 25, D. C. Attn: ReO Re3d
2	Commander Naval Proving Ground Dahlgren, Virginia
2	Commander Naval Ordnance Laboratory White Oak Silver Spring 19, Maryland Attn: Mr. Witt Dr. A.E.Seigel
1	Superintendent Naval Postgraduate School Monterey, California
2	Commander Naval Air Missile Test Center Point Mugu, California
1	Commanding Officer & Director David W. Taylor Model Basin Washington 7, D. C. Attn: Aerodynamics Laboratory

No. of Copies	Organization
1	Commanding Officer Naval Air Rocket Test Station Lake Denmark Dover, New Jersey
1	Commander Naval Air Development Center Johnsville, Pennsylvania
3	Commander Naval Ordnance Test Station China Lake, California Attn: Technical Library Mr. H. L. Newkirk
4	Commander Air Research & Development Command P.O. Box 1395 Baltimore 3, Maryland Attn: Deputy for Development
1	Commander Air Force Armament Center Eglin Air Force Base, Florida Attn: ACOT
1	Commander Arnold Engineering Development Center Tullahoma, Tennessee Attn: Deputy Chief of Staff, R&D
1	Commander USAF Fighter Weapons School Nellis Air Force Base, Nevada Attn: Lt. M.A.Cobra
10	Director Armed Services Technical Information Agency Documents Service Center Knott Building Dayton 2, Ohio Attn: DSC-SD

DISTRIBUTION LIST

No. of Copies	Organization
1	Director National Advisory Committee for Aeronautics 1512 H Street, N.W. Washington 25, D. C.
3	National Advisory Committee for Aeronautics Langley Memorial Aeronautical Laboratory Langley Field, Virginia Attn: Mr. J. Bird Mr. C. E. Brown Dr. Adolf Busemann
1	Director, JPL Ord Corps Installation 4800 Oak Grove Drive Department of the Army Pasadena, California Attn: Mr. Irl E. Newlan
1	Assistant Secretary of Defense (R&E) Pentagon Washington 25, D. C. Attn: Director, Ordnance
1	Commanding Officer Diamond Ordnance Fuze Labs. Washington 25, D. C. Attn: ORDTL 06.33
1	Commanding General Redstone Arsenal Huntsville, Alabama Attn: Technical Library
3	Commanding Officer Picatinny Arsenal Dover, New Jersey Attn: Samuel Feltman Ammunition Labs.
1	Commanding General Frankford Arsenal Philadelphia 37, Pa. Attn: Reports Group
1	Commanding Officer Chemical Corps Chemical & Radiological Laboratory Army Chemical Center, Maryland
1	Commander Lake City Arsenal Independence, Missouri
1	Commanding General Ordnance Ammunition Command Joliet, Illinois
1	Cornell Aeronautical Lab., Inc. 4455 Genesee Street Buffalo 5, New York Attn: Miss Elma T. Evans, Librarian
1	Emerson Electric Mfg., Co. 8100 W. Florissant Avenue St. Louis 21, Missouri Attn: Mr. G. Hauser
1	General Electric Company 1 River Road Schenectady, New York Attn: Mr. F. V. Johnson, A&OE
1	Sperry Gyroscope Company Division of Sperry Corporation Great Neck, Long Island, N. Y. Attn: Mr. J. J. Gallaghan Federal Department
1	Technical Documents Services Willow Run Laboratories University of Michigan Willow Run Airport Ypsilanti, Michigan Attn: Mr. J. E. Corey
1	The University of Texas Military Physics Research Lab. Austin 12, Texas

DISTRIBUTION LIST

No. of Copies	Organization
1	Director National Advisory Committee for Aeronautics 1512 H Street, N.W. Washington 25, D. C.
3	National Advisory Committee for Aeronautics Langley Memorial Aeronautical Laboratory Langley Field, Virginia Attn: Mr. J. Bird Mr. C. E. Brown Dr. Adolf Busemann
1	Director, JPL Ord Corps Installation 4800 Oak Grove Drive Department of the Army Pasadena, California Attn: Mr. Irl E. Newlan
1	Assistant Secretary of Defense (R&E) Pentagon Washington 25, D. C. Attn: Director, Ordnance
1	Commanding Officer Diamond Ordnance Fuze Labs. Washington 25, D. C. Attn: ORDTL 06.33
1	Commanding General Redstone Arsenal Huntsville, Alabama Attn: Technical Library
3	Commanding Officer Picatinny Arsenal Dover, New Jersey Attn: Samuel Feltman Ammunition Labs.
1	Commanding General Frankford Arsenal Philadelphia 37, Pa. Attn: Reports Group
1	Commanding Officer Chemical Corps Chemical & Radiological Laboratory Army Chemical Center, Maryland
1	Commander Lake City Arsenal Independence, Missouri
1	Commanding General Ordnance Ammunition Command Joliet, Illinois
1	Cornell Aeronautical Lab., Inc. 4455 Genesee Street Buffalo 5, New York Attn: Miss Elma T. Evans, Librarian
1	Emerson Electric Mfg., Co. 8100 W. Florissant Avenue St. Louis 21, Missouri Attn: Mr. G. Hauser
1	General Electric Company 1 River Road Schenectady, New York Attn: Mr. F. V. Johnson, A&OE
1	Sperry Gyroscope Company Division of Sperry Corporation Great Neck, Long Island, N. Y. Attn: Mr. J. J. Gallaghan Federal Department
1	Technical Documents Services Willow Run Laboratories University of Michigan Willow Run Airport Ypsilanti, Michigan Attn: Mr. J. E. Corey
1	The University of Texas Military Physics Research Lab. Austin 12, Texas

DISTRIBUTION LIST

No. of Copies	Organization
1	United Shoe Machine Corp. Balch Street Beverly, Massachusetts Attn: Mr. R. S. Parker
1	Wright Aeronautical Division Curtiss-Wright Corporation Wood-Ridge, New Jersey Attn: Sales Dept. (Government)
1	Westinghouse Electric Corp. Air Arm Division Friendship International Airport Baltimore, Maryland
1	Professor George Carrier Division of Applied Sciences Harvard University Cambridge 38, Mass.
1	Professor Clark B. Millikan Guggenheim Aeronautical Lab. California Institute of Technology Pasadena 4, California
1	Dr. A. E. Puckett Hughes Aircraft Company Culver City, California
1	Dr. L. H. Thomas Watson Scientific Computing Laboratory 612 West 116th Street New York 27, New York

ARMY-APG, Md.-D